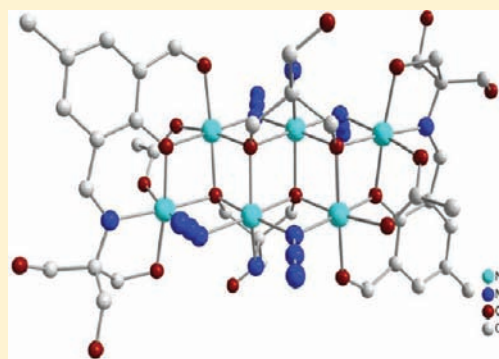


## Structures and Magnetic Properties of an Antiferromagnetically Coupled Polymeric Copper(II) Complex and Ferromagnetically Coupled Hexanuclear Nickel(II) Clusters

Santokh S. Tandon,<sup>\*,†</sup> Scott D. Bunge,<sup>‡</sup> Joaquin Sanchiz,<sup>§</sup> and Laurence K. Thompson<sup>||</sup><sup>†</sup>Department of Chemistry, Kent State University—Salem, Salem, Ohio 44460, United States<sup>‡</sup>Department of Chemistry, Kent State University, Kent, Ohio 44242, United States<sup>§</sup>Departament de Química Inorgànica, Grup d'Interaccions Magnètiques, Universitat de La Laguna, Diagonal 647, 08028, Barcelona, Spain<sup>||</sup>Department of Chemistry, Memorial University, St. John's Newfoundland, A1B 3X7, Canada

## Supporting Information

**ABSTRACT:** Reactions between 2,6-diformyl-4-methylphenol (DFMF) and tris(hydroxymethyl) aminomethane (THMAM = H<sub>3</sub>L<sub>2</sub>) in the presence of copper(II) salts, CuX<sub>2</sub> (X = CH<sub>3</sub>CO<sub>2</sub><sup>-</sup>, BF<sub>4</sub><sup>-</sup>, ClO<sub>4</sub><sup>-</sup>, Cl<sup>-</sup>, NO<sub>3</sub><sup>-</sup>) and Ni(CH<sub>3</sub>CO<sub>2</sub>)<sub>2</sub> or Ni(ClO<sub>4</sub>)<sub>2</sub>/NaC<sub>6</sub>H<sub>5</sub>CO<sub>2</sub>, sodium azide (NaN<sub>3</sub>), and triethylamine (TEA), in one pot self-assemble giving a coordination polymer consisting of repeating pentanuclear copper(II) clusters {[Cu<sub>2</sub>(H<sub>5</sub>L<sup>2-</sup>)(μ-N<sub>3</sub>)<sub>2</sub>][Cu(N<sub>3</sub>)<sub>4</sub>·2CH<sub>3</sub>OH]}<sub>n</sub> (**1**) and hexanuclear Ni(II) complexes [Ni<sub>6</sub>(H<sub>3</sub>L<sup>1-</sup>)<sub>2</sub>(HL<sup>2-</sup>)<sub>2</sub>(μ-N<sub>3</sub>)<sub>4</sub>(CH<sub>3</sub>CO<sub>2</sub>)<sub>2</sub>]·6C<sub>3</sub>H<sub>7</sub>NO·C<sub>2</sub>H<sub>5</sub>OH (**2**) and [Ni<sub>6</sub>(H<sub>3</sub>L<sup>1-</sup>)<sub>2</sub>(HL<sup>2-</sup>)<sub>2</sub>(μ-N<sub>3</sub>)<sub>4</sub>(C<sub>6</sub>H<sub>5</sub>CO<sub>2</sub>)<sub>2</sub>]·3C<sub>3</sub>H<sub>7</sub>NO·3H<sub>2</sub>O·CH<sub>3</sub>OH (**3**). In **1**, H<sub>5</sub>L<sup>2-</sup> and in **2** and **3** H<sub>3</sub>L<sup>1-</sup> and HL<sup>2-</sup> represent doubly deprotonated, singly deprotonated, and doubly deprotonated Schiff-base ligands H<sub>7</sub>L and H<sub>4</sub>L<sup>1</sup> and a tripodal ligand H<sub>3</sub>L<sub>2</sub>, respectively. **1** has a novel double-stranded ladder-like structure in which [Cu<sub>2</sub>(H<sub>5</sub>L<sup>2-</sup>)(μ-N<sub>3</sub>)<sub>2</sub>]<sup>+</sup> anions link single chains comprised of dinuclear cationic subunits [Cu<sub>2</sub>(H<sub>5</sub>L<sup>2-</sup>)(μ-N<sub>3</sub>)<sub>2</sub>]<sup>+</sup>, forming a 3D structure of interconnected ladders through H bonding. Nickel(II) clusters **2** and **3** have very similar neutral hexanuclear cores in which six nickel(II) ions are bonded to two H<sub>4</sub>L<sup>1</sup>, two H<sub>3</sub>L<sub>2</sub>, four μ-azido, and two μ-CH<sub>3</sub>CO<sub>2</sub><sup>-</sup>/μ-C<sub>6</sub>H<sub>5</sub>CO<sub>2</sub><sup>-</sup> ligands. In each structure two terminal dinickel (Ni<sub>2</sub>) units are connected to the central dinickel unit through four doubly bridging end-on (EO) μ-azido and four triply bridging μ<sub>3</sub>-methoxy bridges organizing into hexanuclear units. In each terminal dinuclear unit two nickel centers are bridged through one μ-phenolate oxygen from H<sub>3</sub>L<sup>1-</sup>, one μ<sub>3</sub>-methoxy oxygen from HL<sup>2-</sup>, and one μ-CH<sub>3</sub>CO<sub>2</sub><sup>-</sup> (**2**)/μ-C<sub>6</sub>H<sub>5</sub>CO<sub>2</sub><sup>-</sup> (**3**) ion. Bulk magnetization measurements on **1** show moderately strong antiferromagnetic coupling within the [Cu<sub>2</sub>] building block ( $J_1 = -113.5 \text{ cm}^{-1}$ ). Bulk magnetization measurements on **2** and **3** demonstrate that the magnetic interactions are completely dominated by ferromagnetic coupling occurring between Ni(II) ions for all bridges with coupling constants ( $J_1$ ,  $J_2$ , and  $J_3$ ) ranging from 2.10 to 14.56 cm<sup>-1</sup> (in the  $\hat{H} = -J_1(\hat{S}_1\hat{S}_2) - J_1(\hat{S}_2\hat{S}_3) - J_2(\hat{S}_3\hat{S}_4) - J_1(\hat{S}_4\hat{S}_5) - J_1(\hat{S}_5\hat{S}_6) - J_2(\hat{S}_1\hat{S}_6) - J_3(\hat{S}_2\hat{S}_5) - J_3(\hat{S}_3\hat{S}_5)$  convention).



## INTRODUCTION

Polynuclear spin-coupled coordination clusters of paramagnetic transition metals have been the subject of intensive investigations<sup>1–26</sup> due to their potential applications as single-molecule magnets (SMMs)<sup>1–15</sup> and single-chain magnets (SCMs)<sup>16–21</sup> and in magnetic refrigeration, quantum computing, and the highly competitive area of nanotechnology.<sup>27–29</sup> The number of coordination compounds with a one-dimensional ladder-like, two-dimensional layer, and zigzag ladder-like structures are somewhat rare in the literature.<sup>30–35</sup> In the majority of polymeric coordination complexes in conjunction with the multidentate ligands doubly or triply bridging anions like N<sub>3</sub><sup>-</sup>, NCS<sup>-</sup>, N(CN)<sub>2</sub><sup>-</sup>, CN<sup>-</sup>, C<sub>2</sub>H<sub>3</sub>O<sub>2</sub><sup>-</sup>, C<sub>6</sub>H<sub>5</sub>O<sup>-</sup>, and OH<sup>-</sup> etc., are often used to form extended networks.<sup>36–41</sup> In coordination clusters the nature and magnitude of the magnetic exchange interactions between the

metal centers depend on a number of factors; the most important of these are the type of bridging ligands and bridge angles. Among all, azido and hydroxo (phenoxide and alkoxide) bridges are the most versatile mediators of magnetic exchange interactions between paramagnetic ions due to their flexidentate nature and different modes of coordination.<sup>24,42,43</sup> In most of the reported complexes, azide bridges propagate antiferromagnetic (end-to-end, μ-1,3 bridges) or ferromagnetic interactions (end-on, μ-1,1 bridges) depending upon the nature of the bridges.<sup>24,44</sup> The number of complexes in which azide ions exhibit novel triply bridging (μ<sub>3</sub>-1,1,1 and μ<sub>3</sub>-1,1,3) and quadruple bridging (μ<sub>4</sub>-1,1,1,1 and μ<sub>4</sub>-1,1,3,3) modes is relatively limited.<sup>24,45–52</sup>

Received: December 20, 2011

Published: February 17, 2012

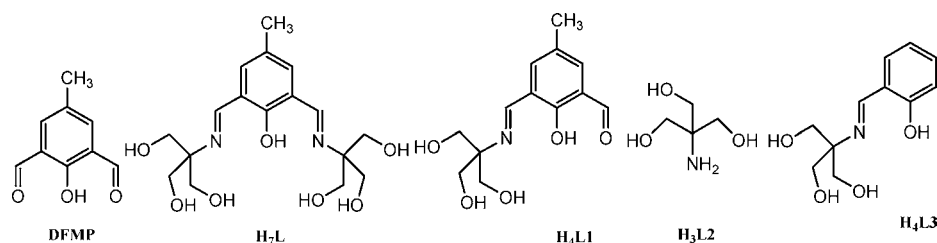


Figure 1. Structures of Schiff-base ligands.

The coordination versatility of the Schiff-base ligand ( $H_4L3$ ) (Figure 1) toward transition metal ions<sup>53–56</sup> has prompted us to synthesize the related ‘double’-Schiff-base ligand  $H_7L$  (Figure 1) and explore its coordination chemistry. It is a potentially ennea-dentate, hepta-anionic ligand with a high degree of conformational flexibility and potential to coordinate in a convergent (directing formation of the dinuclear units) and divergent fashion (ability to extend coordination beyond the primary coordination mode, creating 1-dimensional chain, 2-dimensional sheet, or 3-dimensional structures utilizing one, two, or three protonated/deprotonated hydroxymethyl groups present in each side arm). In a preliminary report<sup>57</sup> we published the structure and magnetism of **1** as a first report with this new ligand. When the same reaction between DFMP (Figure 1) and THMAM was carried out in the presence of nickel(II) salts, condensation occurs only at one end of the DFMP, forming hexanuclear complexes of mono-Schiff-base ligand ( $H_4L1$ ) (Scheme 2).

In a continuation of our interest in the synthesis, structural characterization, and magnetic properties of polynuclear spin-coupled clusters of paramagnetic transition metal ions exhibiting ferromagnetic and antiferromagnetic spin exchange interactions, we explored the coordination chemistry of two new Schiff-base ligands:  $H_7L$ , 2-[(*E*)-(3-[(1*E*)-{[1,3-dihydroxy-2-(hydroxymethyl)propan-2yl]imino}methyl]-2-hydroxy-5-methylphenyl)methylidene)amino]-2-(hydroxymethyl)propane-1,3-diol, potentially an ennea-dentate ( $N_2O_7$ ), hepta-anionic double-Schiff-base, and  $H_4L1$ , 3-[(1*E*)-{[1,3-dihydroxy-2-(hydroxymethyl)propan-2yl]imino}methyl]-2-hydroxy-5-benzaldehyde, potentially a hexa-dentate ( $NO_5$ ), tetra-anionic mono-Schiff-base ligand toward Cu(II) and Ni(II) ions. In this report the synthesis, crystal structures, and magnetic properties of a copper(II) coordination polymer consisting of repeating pentanuclear units  $\{[Cu_2(H_3L^{2-})(\mu-N_3)]_2[Cu(N_3)_4]\cdot 2CH_3OH\}_n$  (**1**) with a novel double-stranded helical ladder-like 3D structure<sup>57</sup> and two hexanuclear nickel(II) clusters are presented. Both Ni(II) complexes **2** and **3** have an essentially identical hexanuclear structural core except that two acetate bridges in **2** are replaced with two benzoate bridges in **3**. In both complexes the basic dinuclear  $[Ni_2]$  units are organized into hexanuclear clusters through a variety of alkoxide, phenoxide, and azide bridges. The magnetic exchange interactions in complexes **2** and **3** are dominated by the moderate ferromagnetic coupling between six nickel(II) centers.

## EXPERIMENTAL SECTION

**Physical Measurements.** Infrared spectra were recorded as Nujol mulls using a Perkin-Elmer FT-IR instrument, and UV–vis spectra of the powdered compounds were obtained as Nujol mulls or in DMF solution using a Cary SE spectrometer. Microanalyses were carried out using a Leco CHNS-Analyzer. Variable-temperature magnetic data (2–300 K) on **1** were obtained using a Quantum Design MPMS3 SQUID magnetometer with a field strength of 0.1 T. Measurements on **2** and **3** were carried out in a similar manner in the temperature

range 1.9–300 K at an applied magnetic field of 0.5 T. Magnetization isotherms were performed at 2 K with applied fields ranging from 0 to 5.0 T. Background corrections for the sample holder assembly and diamagnetic components of the complexes were applied.

**Materials.** 2,6-Diformyl-4-methylphenol (DFMP) was prepared by the reported method,<sup>58</sup> and tris(hydroxymethyl)aminomethane (THMAM) was supplied by Aldrich. All other chemicals used (solvents and metal salts) were analytical or reagent grade and employed without further purification.

**Synthesis of the Coordination Compounds.** **Caution:** Azide and perchlorate complexes of metal ions involving organic ligands are potentially explosive. Only small quantities of the complexes should be prepared, and these should be handled with care.

In some cases there is a significant difference between the most reasonable formula based on elemental analysis (analytical formula) and that obtained from X-ray crystallography. This is evident from the fact that the crystals of these compounds crumble to form powders losing solvents when taken out of the liquids (mother liquors or crystallizing solvents). For consistency, the X-ray formulas will be used throughout the paper. For compound **1**, the X-ray formula is  $\{[Cu_2(H_3L^{2-})(\mu-N_3)]_2[Cu(N_3)_4]\cdot 2CH_3OH\}_n$  and the analysis formula is  $\{[Cu_2(H_3L^{2-})(\mu-N_3)]_2[Cu(N_3)_4]\cdot 2CH_3OH\cdot 2H_2O\}_n$ . For compound **2**, the X-ray formula is  $[Ni_6(H_3L1^-)_2(HL2^{2-})_2(\mu-N_3)_4(CH_3CO_2)_2]\cdot 6C_3H_7NO\cdot C_2H_5OH$  and the analysis formula is  $[Ni_6(H_3L1^-)_2(HL2^{2-})_2(\mu-N_3)_4(CH_3CO_2)_2]\cdot C_2H_5OH\cdot 2H_2O$ . For compound **3**, the X-ray formula is  $[Ni_6(H_3L1^-)_2(HL2^{2-})_2(\mu-N_3)_4(C_6H_5CO_2)_2]\cdot 3C_3H_7NO\cdot 3H_2O\cdot CH_3OH$  and the analysis formula is  $[Ni_6(H_3L1^-)_2(HL2^{2-})_2(\mu-N_3)_4(C_6H_5CO_2)_2]\cdot 2C_3H_7NO\cdot 2H_2O$ . In compounds **1**, **2**, and **3** the CHN analysis shows different solvent ( $C_3H_7NO$  (DMF),  $C_2H_5OH$ ,  $CH_3OH$ ,  $H_2O$ ) molecules compared to X-ray samples as the analysis was carried out on the sample which was just air dried due to its potential explosive nature.

$\{[Cu_2(H_3L^{2-})(\mu-N_3)]_2[Cu(N_3)_4]\cdot 2CH_3OH\}_n$  (**1**). 2,6-Diformyl-4-methylphenol (DFMP) (1.0 mmol, 0.16 g) dissolved in hot methanol (10 mL) was added to a hot methanolic solution (20 mL) of tris(hydroxymethyl)aminomethane (THMAM) (2.0 mmol, 0.24 g) with stirring. A yellow solution of the Schiff-base formed was stirred under reflux for ca. 30 min.  $[Cu_2(O_2CCH_3)_4(H_2O)_2]$  (3.0 mmol, 0.60 g) dissolved in 20 mL of water was added to a solution of the Schiff-base ligand dropwise with stirring under reflux in ca. 10 min. A clear dark green solution obtained was refluxed for ca. 10 min. A solution of sodium azide ( $NaN_3$ ) (4.0 mmol, 0.26 g) in minimum amount of water was added dropwise over a period of 5 min. The reaction mixture (bright dark-green) was stirred under reflux for ca. 3 h, and a small amount of green solid insoluble in all solvents (probably a polymeric complex) was filtered off and discarded. The filtrate was kept undisturbed at ambient temperature. After 1 week dark green crystals of **1** suitable for X-ray study were obtained. Yield: 0.30 g, 43.8%. From the mother liquor a second crop of the compound was also recovered (0.20 g, 29.2%) which showed a very similar IR spectrum:  $\nu(OH)$  at 3580, 3462, 3306  $cm^{-1}$  [uncoordinated methanol groups in the side arms of the double-Schiff-base ligand ( $H_7L$ )],  $\nu N_3$  at 2116, 2078, 2034  $cm^{-1}$  [ $(\mu-1,1-N_3)$ , interdimer bridging azide ( $\mu-1,3-N_3$ ), and terminal  $N_3$ ],<sup>47</sup> and  $\nu(C=N)$  at 1627  $cm^{-1}$  [coordinated imine group]. UV–vis spectrum: strong band at 335 nm and a shoulder at 400 nm [Cu–L charge-transfer and Cu–azide charge-transfer transitions, respectively] and a weak band at 560 nm [d–d transition]. Anal. Calcd for  $\{[Cu_2(H_3L^{2-})N_3]_2[Cu(\mu-N_3)_4]\cdot 2CH_3OH\cdot 2H_2O\}_n$ : C, 30.74; H, 4.30;

N, 21.91. Found: C, 30.23; H, 3.90; N, 21.99. (Note: Elemental analysis shows the presence of two water molecules per pentanuclear unit as water of hydration which are not shown in the X-ray structure).

**1** was also prepared in a very high yield (94.2% based on Schiff-base ligand) by following essentially a similar procedure as described above. This time reaction of  $\text{Cu}(\text{BF}_4)_2 \cdot 3\text{H}_2\text{O}$  (0.90 g, 3.1 mmol) with DFMP (0.16 g, 1.0 mmol) and THMAM (0.24 g, 2.0 mmol) was carried out in methanol (60 mL). After adding a solution of  $\text{NaN}_3$  (0.40 g, 6.0 mmol) in a mixture of methanol:water (3 + 1 mL), the dark green clear solution produced was filtered and the filtrate was left undisturbed at ambient temperature for slow evaporation. After about 48 h, dark green needles separated in a brownish-green solution were filtered off, washed with methanol ( $2 \times 3$  mL), and dried in air (yield 0.68 g, 94.2%). Single-crystal X-ray determination on this sample showed this to be exactly identical to the structure of **1**. Similar results were obtained when the reaction was carried out with  $\text{Cu}(\text{ClO}_4)_2 \cdot 6\text{H}_2\text{O}$ .

When the above reaction was carried out with  $\text{CuCl}_2 \cdot 2\text{H}_2\text{O}$  or  $\text{Cu}(\text{NO}_3)_2 \cdot 3\text{H}_2\text{O}$  in the presence of sodium benzoate ( $\text{NaC}_6\text{H}_5\text{CO}_2$ ) under similar conditions as described for  $\text{Cu}(\text{BF}_4)_2 \cdot 3\text{H}_2\text{O}$ , **1** was obtained in very high yield (80.3%). X-ray structure determination on this complex showed it to be identical to **1**. The filtrate from the  $\text{Cu}(\text{NO}_3)_2 \cdot 3\text{H}_2\text{O}/\text{NaC}_6\text{H}_5\text{CO}_2$  reaction on standing for a few days formed bluish-green needles. X-ray structure determination showed this to be a dinuclear Cu(II) complex  $[\text{Cu}_2(\text{C}_6\text{H}_5\text{CO}_2)_4(\text{C}_2\text{H}_5\text{OH})_2] \cdot 2.5\text{H}_2\text{O}$ , which has already been reported.<sup>59</sup> Anal. Calcd for  $[\text{Cu}_2(\text{C}_6\text{H}_5\text{CO}_2)_4(\text{C}_2\text{H}_5\text{OH})_2] \cdot 2.5\text{H}_2\text{O}$ : C, 51.33; H, 4.98. Found: C, 51.05; H, 4.47.

**$[\text{Ni}_6(\text{H}_3\text{L}1^-)_2(\text{HL}2^{2-})_2(\mu\text{-N}_3)_4(\text{CH}_3\text{CO}_2)_2] \cdot 6\text{C}_3\text{H}_7\text{NO} \cdot \text{C}_2\text{H}_5\text{OH}$  (2).** DFMP (0.16 g, 1.0 mmol) dissolved in hot methanol (15 mL) was added to a solution of THMAM (0.24 g, 2.0 mmol) in the same solvent (15 mL). The yellow solution of the Schiff-base ligand formed was stirred under reflux for ca. 60 min.  $\text{Ni}(\text{CH}_3\text{CO}_2)_2 \cdot 4\text{H}_2\text{O}$  (0.80 g, 3.2 mmol) dissolved in an ethanol:methanol mixture (10 + 10 mL) was added to the solution of the Schiff-base ligand dropwise with stirring under reflux. The resulting green solution was refluxed further for ca. 20 min, and a solution of triethylamine (TEA) (0.22 g, 2.2 mmol) in 10 mL of ethanol was added dropwise. After refluxing the reaction mixture for another 10 min. A solution of  $\text{NaN}_3$  (0.26 g, 4.0 mmol) in an ethanol:water mixture (8 + 2 mL) was added dropwise. The color of the reaction mixture changed to dark green, and the solution was refluxed further for ca. 1.5 h, concentrated to ca. 20 mL, and filtered hot. The filtrate was left unperturbed for slow evaporation. After about 2 weeks, a green solid separated in a green solution was filtered off, washed with methanol ( $2 \times 3$  mL), and air dried. Crystals suitable for X-ray studies were obtained by slow diffusion of diethyl ether into a solution of the complex in a mixture of dimethylformamide (DMF), methanol, and ethanol. Yield: 0.25 g, 34.0%, based on DFMP. A second crop (0.25 g, 34.0%), recovered from the mother liquor, has an identical IR spectrum: two strong bands at 2080 and 2051 [ $\nu(\mu\text{-}1,1\text{-N}_3)$  of slightly asymmetric bridging azides], strong bands at 3467, 3345, 3286, and 3221 [ $\nu\text{OH}$  of uncoordinated methanol groups in the side arms of  $\text{H}_4\text{L}1$  and  $\text{H}_3\text{L}2$  ligands], two strong bands at 1658 and 1642 [ $\nu\text{CO}_2^-$  of coordinated acetate], and 1621  $\text{cm}^{-1}$  [ $\nu(\text{C}=\text{N})$ ]. UV-vis spectrum: 382 and 265 [Ni-azide and Ni-L charge-transfer transitions, respectively] and 595 nm [d-d transition characteristic of octahedrally based geometry]. Anal. Calcd for  $[\text{Ni}_6(\text{H}_3\text{L}1^-)_2(\text{HL}2^{2-})_2(\mu\text{-N}_3)_4(\text{CH}_3\text{CO}_2)_2] \cdot 2\text{C}_2\text{H}_5\text{OH} \cdot 2\text{H}_2\text{O}$ : C, 32.22; H, 4.46; N, 15.03 (air-dried X-ray sample). Found: C, 31.99; H, 4.72; N, 15.18.

**$[\text{Ni}_6(\text{H}_3\text{L}1^-)_2(\text{HL}2^{2-})_2(\mu\text{-N}_3)_4(\text{C}_6\text{H}_5\text{CO}_2)_2] \cdot 3\text{C}_3\text{H}_7\text{NO} \cdot 3\text{H}_2\text{O} \cdot \text{CH}_3\text{OH}$  (3).** Compound **3** was prepared using exactly the same procedure as used for **2** by replacing  $\text{Ni}(\text{CH}_3\text{CO}_2)_2 \cdot 4\text{H}_2\text{O}$  with  $\text{Ni}(\text{ClO}_4)_2 \cdot 6\text{H}_2\text{O}/\text{NaC}_6\text{H}_5\text{CO}_2$ . In this case, after adding  $\text{NaN}_3$  dissolved in a water + methanol (1 + 5 mL) mixture followed by sodium benzoate ( $\text{NaC}_6\text{H}_5\text{CO}_2$ ) (0.30 g, 2.0 mmol) dissolved in 3.0 mL of water, the reaction mixture was refluxed for ca. 1.5 h. The bright green solution formed was filtered, and the filtrate was left undisturbed for slow evaporation. After 3 weeks the green solid separated was filtered off, washed with methanol ( $2 \times 3$  mL), and air dried. Crystals suitable for X-ray analysis were obtained by dissolving the solid in a minimum quantity of hot DMF and adding an equivalent amount of methanol.

After keeping the solution (closed) at room temperature for about 1 week X-ray-quality crystals were obtained. Yield: 0.66 g, 77.0%, based on DFMP. IR spectrum: two strong bands at 2080 and 2051 [ $\nu(\mu\text{-}1,1\text{-N}_3)$  of slightly asymmetric bridging azides],<sup>47</sup> three strong bands at 3450, 3356, and 3290 [ $\nu\text{OH}$  of uncoordinated methanol groups in the side arms of  $\text{H}_4\text{L}1$  and  $\text{H}_3\text{L}2$  ligands], a strong band at 1643 [ $\nu\text{CO}_2^-$  of coordinated benzoate], and 1622  $\text{cm}^{-1}$  [ $\nu(\text{C}=\text{N})$ ]. UV-vis spectrum: 380 and 263 [Ni-azide and Ni-L charge-transfer transitions, respectively] and 595 nm [d-d transition characteristic of octahedrally based geometry]. Anal. Calcd for  $[\text{Ni}_6(\text{H}_3\text{L}1^-)_2(\text{HL}2^{2-})_2(\mu\text{-N}_3)_4(\text{C}_6\text{H}_5\text{CO}_2)_2] \cdot 2\text{C}_3\text{H}_7\text{NO} \cdot 2\text{H}_2\text{O}$  on the air-dried X-ray and magnetic sample: C, 37.81; H, 4.58; N, 14.70. Found: C, 37.91; H, 4.64; N, 15.03.

**X-ray Crystallography.** Crystal data of compounds **1–3** were collected by exactly the same method, by mounting a crystal onto a thin glass fiber and immediately placing under a liquid  $\text{N}_2$  cooled  $\text{N}_2$  stream, on a Bruker AXS platform single-crystal X-ray diffractometer upgraded with an APEX II CCD detector. The radiation used is graphite-monochromatized Mo  $K\alpha$  radiation ( $\lambda = 0.7107 \text{ \AA}$ ). Lattice parameters are optimized from a least-squares calculation on carefully centered reflections. Lattice determination, data collection, data reduction, and structure refinement were carried out using the APEX2 Version 1.0-27 software package.<sup>60,61</sup> Data were corrected for absorption using the SCALE program within the APEX2 software package.<sup>60,61</sup> Structures were solved using direct methods. This procedure yielded the Cu or Ni atoms, along with a number of the C, N, and O atoms. Subsequent Fourier synthesis yielded the remaining atom positions. Hydrogen atoms are fixed in positions of ideal geometry (riding model) and refined within the XSELL software package.<sup>62</sup> These idealized hydrogen atoms had their isotropic temperature factors fixed at 1.2 or 1.5 times the equivalent isotropic U of the C atoms to which they were bonded. A few hydrogen atoms could not be adequately predicted via the riding model within the XSELL software.<sup>62</sup> These hydrogen atoms were located via difference Fourier mapping and subsequently refined. The final refinement of each compound included anisotropic thermal parameters on all non-hydrogen atoms. Crystal data for compounds **1–3** are given in Table 1. Selected interatomic distances and bond angles are listed in Tables 2–4.

**Table 1. Summary of Crystallographic Data for Compounds 1–3**

	1	2	3
empirical formula	$\text{C}_{36}\text{H}_5\text{Cu}_3\text{N}_{22}\text{O}_{16}$	$\text{C}_{58}\text{H}_{104}\text{N}_{22}\text{Ni}_6\text{O}_{27}$	$\text{C}_{113}\text{H}_{160}\text{N}_{40}\text{Ni}_{12}\text{O}_{45}$
<i>M</i>	1366.70	1893.89	3503.33
cryst syst	monoclinic	monoclinic	triclinic
space group	<i>C</i> 2/ <i>c</i>	<i>P</i> 2 <sub>1</sub> / <i>c</i>	<i>P</i> -1
<i>a</i> /Å	23.219(4)	18.6655(8)	13.1039(9)
<i>b</i> /Å	8.0004(12)	13.5651(5)	14.0634(15)
<i>c</i> /Å	29.702(4)	17.0577(7)	21.9161(15)
$\alpha$ /deg			84.9980(10)
$\beta$ /deg	108.004(2)	103.8480(10)	88.4770(10)
$\gamma$ /deg			64.3330(10)
<i>V</i> /Å <sup>3</sup>	5247.3(14)	4193.5(3)	3626.1(4)
$\rho_{\text{calcd}}$ (g cm <sup>-3</sup> )	1.730	1.500	1.604
<i>T</i> /K	100(2)	189(2)	186(2)
<i>Z</i>	4	2	1
$\mu$ /mm <sup>-1</sup>	2.081	1.405	1.613
cryst size (mm)	0.30 × 0.20 × 0.10	0.15 × 0.14 × 0.10	0.32 × 0.28 × 0.25
total reflns collected	20 501	33 235	29 537
unique reflns collected	4661	7425	12 817
<i>R</i> <sub>int</sub>	0.0317	0.0582	0.0362
final <i>R</i> <sub>1</sub> , <i>wR</i> <sub>2</sub> <sup>a</sup>	0.0332, 0.1054	0.0426, 0.1244	0.0596, 0.1782

$$^a R_1 = \frac{\sum [ |F_o| - |F_c| ]}{\sum |F_o|}, wR_2 = \frac{[\sum w(|F_o|^2 - |F_c|^2)^2]}{[\sum w(|F_o|^2)^2]}^{1/2}, R = \frac{\sum ||F_o| - |F_c||}{\sum |F_o|}, R_w = \frac{[\sum w(|F_o| - |F_c|)^2]}{\sum w|F_o|^2}^{1/2}.$$



**Table 2. Bond Lengths [Angstroms] and Angles [degrees] for 1**

bond lengths		bond angles	
Cu(1)–O(5)	1.8888(17)	O(5)–Cu(1)–N(2)	85.68(8)
Cu(1)–N(2)	1.931(2)	O(5)–Cu(1)–O(1)	172.80(8)
Cu(1)–O(1)	1.9319(17)	N(2)–Cu(1)–O(1)	92.86(8)
Cu(1)–N(3)	1.992(2)	O(5)–Cu(1)–N(3)	101.08(8)
Cu(1)–N(11)	2.569(3)	N(2)–Cu(1)–N(3)	172.71(8)
Cu(2)–O(2)	1.9178(17)	O(1)–Cu(1)–N(3)	80.09(8)
Cu(2)–N(1)	1.926(2)	O(2)–Cu(2)–N(1)	85.86(8)
Cu(2)–O(1)	1.9394(17)	O(2)–Cu(2)–O(1)	171.17(8)
Cu(2)–N(3)	1.984(2)	N(1)–Cu(2)–O(1)	93.22(8)
Cu(3)–N(8)	1.968(2)	O(2)–Cu(2)–N(3)	99.91(8)
Cu(3)–N(8A)	1.968(2)	N(1)–Cu(2)–N(3)	171.51(8)
Cu(3)–N(9A)	1.970(3)	O(1)–Cu(2)–N(3)	80.12(8)
Cu(3)–N(9)	1.970(3)	N(8)–Cu(3)–N(8A)	180.00(10)
		N(8)–Cu(3)–N(9A)	89.03(11)
		N(8A)–Cu(3)–N(9A)	90.97(11)
		N(8)–Cu(3)–N(9)	90.97(11)
		N(8A)–Cu(3)–N(9)	89.03(11)
		N(9A)–Cu(3)–N(9)	180.0(2)
		C(5)–O(1)–Cu(1)	128.68(15)
		C(5)–O(3)–Cu(2)	128.51(15)
		Cu(1)–O(1)–Cu(2)	101.61(8)
		N(4)–N(3)–Cu(2)	128.18(16)
		N(4)–N(3)–Cu(1)	127.15(17)
		Cu(2)–N(3)–Cu(1)	97.97(9)

## RESULTS AND DISCUSSION

**Synthesis of the Complexes.** A preliminary report<sup>57</sup> on the structure and some properties of compound **1** with a new very versatile double-Schiff-base ligand ( $H_7L$ ) with a high degree of conformational flexibility has already appeared. In a continuation of our further investigation on the coordination potential of  $H_7L$ , we undertook a systematic approach and carried out a series of reactions between DFMP and THMAM in the presence of several copper(II) and nickel(II) salts under varied reaction conditions to investigate the effects of various anions ( $Cl^-$ ,  $NO_3^-$ ,  $CH_3CO_2^-$ ,  $ClO_4^-$ ,  $BF_4^-$ ) and transition metals on formation and coordinating abilities of a new Schiff-base ligand ( $H_7L$ ). Earlier<sup>63,64</sup> we have seen that the nature of the anions and the metal ions have remarkable effects on formation of the ligand and self-assembly of polynuclear metal clusters of similar Schiff-base ligands. Regardless of the copper salt [ $CuCl_2$ ,  $Cu(BF_4)_2$ ,  $Cu(ClO_4)_2$ ,  $[Cu_2(O_2CCH_3)_4(H_2O)_2]$ ,  $Cu(NO_3)_2/NaC_6H_5CO_2$ ] and the reaction conditions used (room temperature or stirring under reflux for up to 3.5 h in the presence or absence of triethylamine), reaction of DFMP with THMAM, copper(II) salt, and  $NaN_3$  in methanol, methanol/ethanol, or methanol/water mixtures always result in formation of a polymeric coordination complex comprised of repeating pentanuclear copper(II) clusters **1** (Scheme 1) of a double-Schiff-base ligand ( $H_7L$ ) which organizes through self-assembly into unprecedented double-stranded ladder-like structure. This clearly demonstrates that of all the possible products complex **1** is kinetically and thermodynamically the most stable and most favored product. To the best of our knowledge,  $H_7L$  is a new ligand and **1** seems to be the first complex of this ligand (CCDC Search).

Reactions between DFMP and THMAM in the presence of  $Ni(CH_3CO_2)_2$  and  $Ni(ClO_4)_2/NaC_6H_5CO_2$ ,  $NaN_3$ , and TEA in methanol/water or methanol/ethanol/water mixtures produce hexanickel complexes **2** and **3**, respectively (Scheme 2), of

**Table 3. Bond Lengths [Angstroms] and Angles [degrees] for 2**

bond lengths		bond angles	
Ni(1)–O(7)	2.020(2)	O(7)–Ni(1)–N(6)	176.35(11)
Ni(1)–N(6)	2.055(3)	O(7)–Ni(1)–O(9A)	81.48(9)
Ni(1)–O(9A)	2.067(2)	N(6)–Ni(1)–O(9A)	96.47(11)
Ni(1)–O(9)	2.073(2)	O(7)–Ni(1)–O(9)	92.70(9)
Ni(1)–N(2)	2.095(3)	N(6)–Ni(1)–N(9)	83.98(11)
Ni(1)–N(5)	2.112(3)	O(9A)–Ni(1)–O(9)	81.27(10)
Ni(2)–O(4)	2.014(2)	O(7)–Ni(1)–N(2)	82.57(11)
Ni(2)–N(1)	2.017(3)	N(6)–Ni(1)–N(2)	100.75(12)
Ni(2)–O(7A)	2.031(2)	O(9A)–Ni(1)–N(2)	98.20(10)
Ni(2)–O(6)	2.062(3)	O(9)–Ni(1)–N(2)	175.26(10)
Ni(2)–O(3)	2.081(3)	O(7)–Ni(1)–N(5)	80.45(11)
Ni(2)–N(2A)	2.135(3)	N(6)–Ni(1)–N(5)	100.35(13)
Ni(3)–O(4)	2.026(2)	O(9A)–Ni(1)–N(5)	152.23(11)
Ni(3)–O(7A)	2.039(2)	O(9)–Ni(1)–N(5)	78.72(11)
Ni(3)–N(6)	2.048(3)	N(2)–Ni(1)–N(5)	100.15(13)
Ni(3)–O(5)	2.051(2)	O(4)–Ni(2)–N(1)	91.02(11)
Ni(3)–O(1)	2.052(3)	O(4)–Ni(2)–O(7A)	85.90(9)
Ni(3)–O(9)	2.066(2)	N(1)–Ni(2)–O(7A)	176.70(11)
Ni(1)–Ni(2)	3.122	O(4)–Ni(2)–O(6)	90.06(10)
Ni(1)–Ni(3)	3.106	N(1)–Ni(2)–N(6)	90.95(11)
Ni(2)–Ni(3)	2.9409(6)	O(7A)–Ni(2)–O(6)	87.88(9)
Ni(1)–Ni(1A)	3.142	O(4)–Ni(2)–O(3)	173.43(10)
Ni(1A)–Ni(3)	3.059	N(1)–Ni(2)–O(3)	82.47(11)
		O(7)–Ni(2)–O(3)	100.60(10)
		O(6)–Ni(1)–O(3)	89.20(10)
		O(4)–Ni(2)–N(2A)	89.84(11)
		N(1)–Ni(2)–N(2A)	99.84(12)
		O(7A)–Ni(2)–N(2A)	81.35(10)
		O(6)–Ni(2)–N(2A)	169.20(11)
		O(3)–Ni(2)–N(2A)	92.11(11)
		O(4)–Ni(3)–O(7A)	85.38(9)
		O(4)–Ni(3)–N(6)	174.99(11)
		O(7A)–Ni(3)–N(6)	95.21(11)
		O(4)–Ni(3)–O(5)	88.11(10)
		O(7A)–Ni(3)–O(5)	91.02(9)
		N(6)–Ni(3)–O(5)	96.86(11)
		O(4)–Ni(3)–O(1)	87.73(10)
		O(7A)–Ni(3)–O(1)	172.13(10)
		N(6)–Ni(3)–O(1)	91.32(11)
		O(5)–Ni(3)–O(1)	92.56(10)
		O(4)–Ni(3)–O(9)	90.85(9)
		O(7A)–Ni(3)–O(9)	81.07(9)
		N(6)–Ni(3)–O(9)	84.33(11)
		O(5)–Ni(3)–O(9)	172.07(10)
		O(1)–Ni(3)–O(9)	95.25(10)

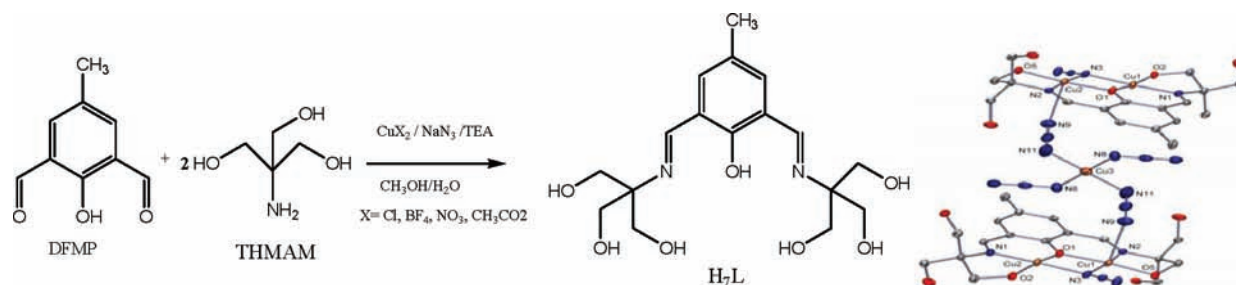
a new single-Schiff-base ligand ( $H_4L1$ ) formed by 1 + 1 condensation rather than 1 + 2 condensation observed in **1**. Formation of a single-Schiff-base ligand ( $H_4L1$ ) present in **2** and **3** contrary to a double-Schiff-base ligand ( $H_7L$ ) formed in **1** can be assigned to presumably either the nickel(II)-assisted partial hydrolysis of one of the two arms of an initially formed double-Schiff-base ligand ( $H_7L$ )<sup>65</sup> or preferential stereochemical requirements of nickel(II) metal centers in hexanuclear units.<sup>64</sup> Recently Ray et al.<sup>65</sup> reported partial hydrolysis of one of the arms of a similar double-Schiff-base ligand ( $H_3L$ , formed by 1 + 2 condensation of DFMP and 2-aminoethanol) in a hexanickel ( $Ni^{II}_6$ ) cluster involving two double-Schiff-base ligands, two single-Schiff-base ligands, and azido bridges. In

**Table 4. Bond Lengths [Angstroms] and Angles [degrees] for 3**

bond lengths		bond angles	
Ni(1)–O(7)	2.020(2)	O(7)–Ni(1)–N(6)	176.35(11)
Ni(1)–N(6)	2.055(3)	O(7)–Ni(1)–O(9A)	81.48(9)
Ni(1)–O(9A)	2.067(2)	N(6)–Ni(1)–O(9A)	96.47(11)
Ni(1)–O(9)	2.073(2)	O(7)–Ni(1)–O(9)	92.70(9)
Ni(1)–N(2)	2.095(3)	N(6)–Ni(1)–N(9)	83.98(11)
Ni(1)–N(5)	2.112(3)	O(9A)–Ni(1)–O(9)	81.27(10)
Ni(2)–O(4)	2.014(2)	O(7)–Ni(1)–N(2)	82.57(11)
Ni(2)–N(1)	2.017(3)	N(6)–Ni(1)–N(2)	100.75(12)
Ni(2)–O(7A)	2.031(2)	O(9A)–Ni(1)–N(2)	98.20(10)
Ni(2)–O(6)	2.062(3)	O(9)–Ni(1)–N(2)	175.26(10)
Ni(2)–O(3)	2.081(3)	O(7)–Ni(1)–N(5)	80.45(11)
Ni(2)–N(2A)	2.135(3)	N(6)–Ni(1)–N(5)	100.35(13)
Ni(3)–O(4)	2.026(2)	O(9A)–Ni(1)–N(5)	152.23(11)
Ni(3)–O(7A)	2.039(2)	O(9)–Ni(1)–N(5)	78.72(11)
Ni(3)–N(6)	2.048(3)	N(2)–Ni(1)–N(5)	100.15(13)
Ni(3)–O(5)	2.051(2)	O(4)–Ni(2)–N(1)	91.02(11)
Ni(3)–O(1)	2.052(3)	O(4)–Ni(2)–O(7A)	85.90(9)
Ni(3)–O(9)	2.066(2)	N(1)–Ni(2)–O(7A)	176.70(11)
Ni(1)–Ni(2)	3.122	O(4)–Ni(2)–O(6)	90.06(10)
Ni(1)–Ni(3)	3.106	N(1)–Ni(2)–N(6)	90.95(11)
Ni(2)–Ni(3A)	2.941	O(7A)–Ni(2)–O(6)	87.88(9)
		O(4)–Ni(2)–O(3)	173.43(10)
		N(1)–Ni(2)–O(3)	82.47(11)
		O(7)–Ni(2)–O(3)	100.60(10)
		O(6)–Ni(1)–O(3)	89.20(10)
		O(4)–Ni(2)–N(2A)	89.84(11)
		N(1)–Ni(2)–N(2A)	99.84(12)
		O(7A)–Ni(2)–N(2A)	81.35(10)
		O(6)–Ni(2)–N(2A)	169.20(11)
		O(3)–Ni(2)–N(2A)	92.11(11)
		O(4)–Ni(3)–O(7A)	85.38(9)
		O(4)–Ni(3)–N(6)	174.99(11)
		O(7A)–Ni(3)–N(6)	95.21(11)
		O(4)–Ni(3)–O(5)	88.11(10)
		O(7A)–Ni(3)–O(5)	91.02(9)
		N(6)–Ni(3)–O(5)	96.86(11)
		O(4)–Ni(3)–O(1)	87.73(10)
		O(7A)–Ni(3)–O(1)	172.13(10)
		N(6)–Ni(3)–O(1)	91.32(11)
		O(5)–Ni(3)–O(1)	92.56(10)
		O(4)–Ni(3)–O(9)	90.85(9)
		O(7A)–Ni(3)–O(9)	81.07(9)
		N(6)–Ni(3)–O(9)	84.33(11)
		O(5)–Ni(3)–O(9)	172.07(10)
		O(1)–Ni(3)–O(9)	95.25(10)

our earlier communications,<sup>63,64</sup> we also reported formation of hexanickel ( $\text{Ni}^{\text{II}}_6$ ) clusters involving two double-Schiff-base ( $\text{H}_3\text{L}$ ) ligands, two single-Schiff-base ligands, and azido bridges and tetranickel ( $\text{Ni}^{\text{II}}_4$ ), tetracopper ( $\text{Cu}^{\text{II}}_4$ ), and mixed-valence tetracobalt ( $\text{Co}_2^{\text{II}}\text{Co}_2^{\text{III}}$ ) clusters involving only two double-Schiff-base ligands ( $\text{H}_3\text{L}$ ) and methoxy, acetate, and azido bridges depending upon the nature of the anions and metal ions used. In hexanickel ( $\text{Ni}^{\text{II}}_6$ ) clusters formation of a single-Schiff-base ligand along with double-Schiff-base ligands was assigned to the preferential stereochemical requirements of the nickel(II) centers in hexanuclear units which was not observed in copper, cobalt, or manganese clusters.<sup>63,64,66,67</sup> From these investigations it appears that the single-Schiff-base ligands are formed (either by nickel-catalyzed partial hydrolysis or by preferential 1 + 1 condensation) only when hexanickel clusters are produced. To this point we have not been able to isolate any tetranuclear or a hexanuclear nickel(II) clusters involving double-Schiff-base ligand ( $\text{H}_3\text{L}$ ) contrary to what was observed with analogous double-Schiff-base ligand ( $\text{H}_3\text{L}$ ).<sup>64</sup>

**Description of Structures.**  $\{[\text{Cu}_2(\text{H}_5\text{L})^{2-}(\mu\text{-N}_3)]_2[\text{Cu}(\text{N}_3)_4] \cdot 2\text{CH}_3\text{OH}\}_n$  (**1**). Complex **1** is obtained as a major product by reacting DFMP and THMAM in the presence of copper(II) salts  $[\text{CuCl}_2, \text{Cu}(\text{BF}_4)_2, \text{Cu}(\text{ClO}_4)_2, [\text{Cu}_2(\text{O}_2\text{CCH}_3)_4(\text{H}_2\text{O})_2], \text{Cu}(\text{NO}_3)_2/\text{C}_6\text{H}_5\text{CO}_2^-]$  and sodium azide ( $\text{NaN}_3$ ) in a methanol:water mixture. Single-crystal X-ray diffraction study reveals that the structure of **1** consists of one-dimensional zigzag single chains resulting from the bridging of the dinuclear units  $[\text{Cu}_2(\text{H}_5\text{L})(\mu\text{-N}_3)]^+$  through methoxy links in the side arm of the Schiff-base ligands ( $\text{H}_5\text{L}^{2-}$ ), and these chains are bridged through  $[\text{Cu}(\text{N}_3)_4]^{2-}$  anions forming double-helical ladders. The molecular structure of complex **1** is shown in Figure 2, together with relevant atomic labeling. Important bond distances and bond angles are listed in Table 2. In complex **1**,  $\text{H}_7\text{L}$  acts as a hexadentate ( $\text{N}_2\text{O}_4$ ) dianionic ligand ( $\text{H}_5\text{L}^{2-}$ ) binding two copper centers in close proximity, forming dinuclear  $[\text{Cu}_2]$  subunits. The overall molecular structure of **1** consists of two zigzag single chains connected by square planar tetra-azido copper(II) anions,  $[\text{Cu}(\text{N}_3)_4]^{2-}$ , producing an unprecedented double-stranded ladder (Figure 2). Each single chain is comprised of repeating dinuclear, 1,1-azido-bridged cationic subunits,  $[(\text{H}_5\text{L})^{2-}\text{Cu}_2(\mu\text{-N}_3)]^+$ , interconnected through a protonated hydroxymethyl oxygen of the side arm of the Schiff-base ligand to form zigzag single chains along the *b* axis. The structure of a repeating pentanuclear subunit  $\{[(\text{H}_5\text{L}^{2-})\text{Cu}_2(\mu\text{-N}_3)]_2[\text{Cu}(\text{N}_3)_4] \cdot 2\text{CH}_3\text{OH}\}$ , which is comprised of two dinuclear cationic units  $[(\text{H}_5\text{L}^{2-})\text{Cu}_2(\mu\text{-N}_3)]^+$ , one from each chain and linked through mononuclear  $[\text{Cu}(\text{N}_3)_4]^{2-}$  anions is shown in Figure 3. Within each pentanuclear unit there are

**Scheme 1. Reactions between DFMP and THMAM in the Presence of Cu(II) Salts Form Pentanuclear Complex 1 of a Double-Schiff-Base Ligand  $\text{H}_7\text{L}$** 

Scheme 2. Reactions between DFMP and THMAM in the Presence of Ni(II) Salts Produce Hexanuclear Complexes 2 and 3 of a Schiff-Base Ligand H<sub>4</sub>L1

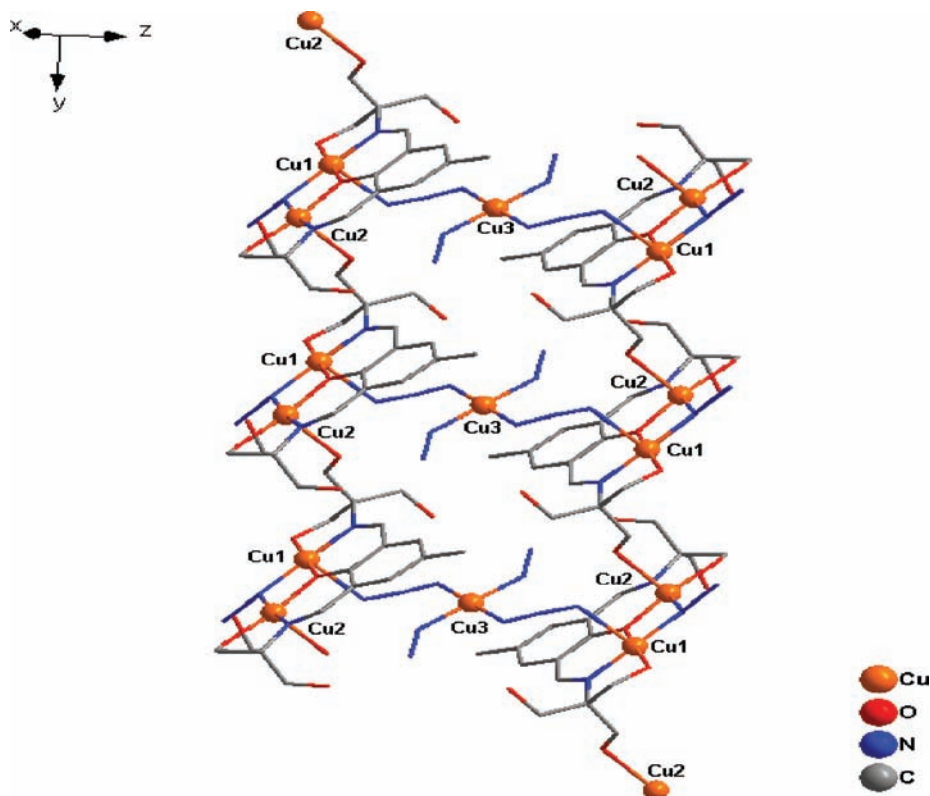
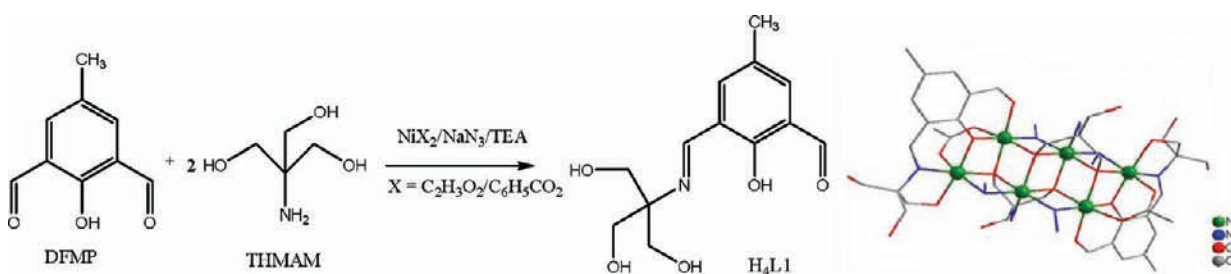


Figure 2. Molecular structure of a double-stranded one-dimensional ladder in **1** along the *b* axis.

intramolecular hydrogen-bonding connections between free hydroxymethyl groups of the side arms of the ligand and the azide groups of the  $[\text{Cu}(\text{N}_3)_4]^{2-}$  anions, providing extra interactions, which hold the chains together in ladders (Figure 3). The ladders are interconnected along the *a*, *c* axes through interladder H bonding, forming the novel 3D structure (Figure 4).

Within each dinuclear subunit, H<sub>7</sub>L acts as a pentadentate ( $\text{N}_2\text{O}_3$ ) dianionic ligand ( $\text{H}_5\text{L}^{2-}$ ) in a convergent fashion, holding two copper ions very tightly in the dinuclear pocket (Figure 3), resulting in a double (phenolate oxygen and end-on (EO) azide ( $\mu\text{-N}_1\text{N}_1$ )) bridged structure. On the basis of reported data, the phenoxide ( $\text{Cu}(1)\text{-O}(1)\text{-Cu}(2) = 101.61(8)^\circ$ ) and azide ( $\text{Cu}(1)\text{-N}(3)\text{-Cu}(2) = 97.97(9)^\circ$ ) bridge angles suggest the presence of antiferromagnetic and ferromagnetic exchange interactions, respectively, between copper centers.<sup>68</sup> The stereochemical arrangements around Cu(1) and Cu(2) in the basal plane are planar. This leads to only axial sites being available, which is why the subunits link up, forming single chains and double-stranded ladders. The square pyramidal geometries at

these metal centers are completed with an azide nitrogen (N(11)) from the central anionic species  $[\text{Cu}(\text{N}_3)_4]^{2-}$  occupying one axial site at Cu(1) and one pendant hydroxymethyl oxygen (O(7)) occupying the axial position on Cu(2). The Cu(1)–Cu(2) distance of 3.000 Å is quite normal for dinuclear copper(II) units of this type.<sup>63</sup>

$[\text{Ni}_6(\text{H}_3\text{L}1^-)_2(\text{HL}2^{2-})_2(\mu\text{-N}_3)_4(\text{CH}_3\text{CO}_2)_2] \cdot 6\text{C}_3\text{H}_7\text{NO} \cdot \text{C}_2\text{H}_5\text{OH}$  (**2**) and  $[\text{Ni}_6(\text{H}_3\text{L}1^-)_2(\text{HL}2^{2-})_2(\mu\text{-N}_3)_4(\text{C}_6\text{H}_5\text{CO}_2)_2] \cdot 3\text{C}_3\text{H}_7\text{NO} \cdot 3\text{H}_2\text{O} \cdot \text{CH}_3\text{OH}$  (**3**). Single-crystal X-ray analysis shows that compounds **2** and **3** have similar structural cores and are isostructural. The only difference between **2** and **3** is the presence of bridging benzoate groups in **3** instead of the bridging acetate groups for **2** and the presence of two slightly different hexanickel molecules in the unit cell of compound **3**. The structures of **2** and **3** can best be described either as a dimer of two trinuclear subunits bridged through two triply bridging alkoxy oxygen ( $\mu_3\text{-O}$ ) and two doubly bridging end-on (EO) azido ( $\mu\text{-N}_3$ ) bridges or a central dinuclear unit ( $\text{Ni}_2$ ) connected to two terminal dinuclear units ( $\text{Ni}_2$ ) to form hexanuclear ( $\text{Ni}_6$ ) clusters. We will use the second approach to describe these structures.



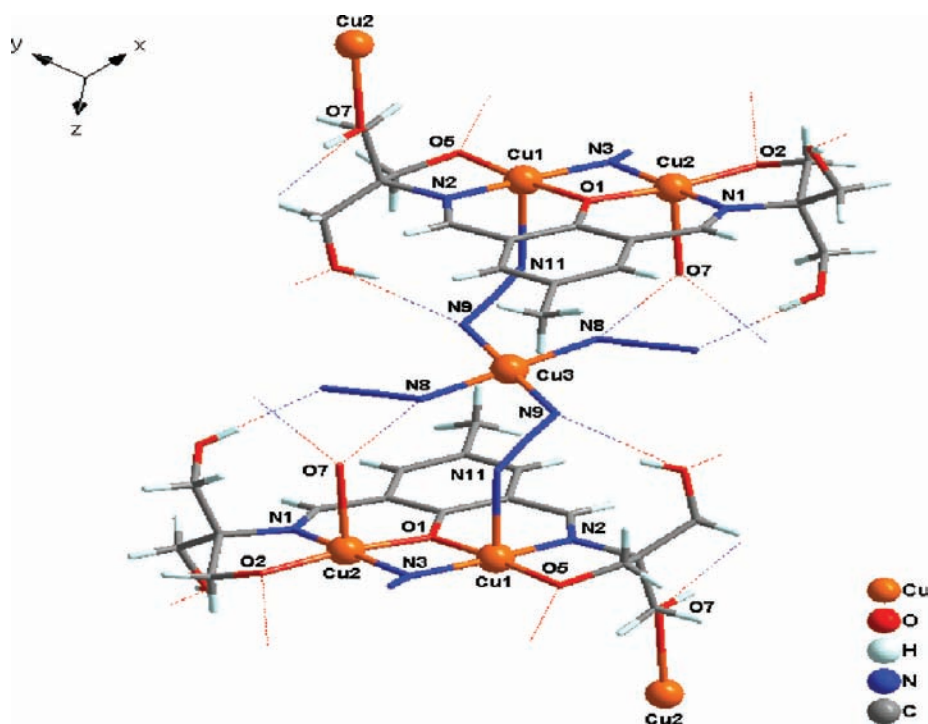


**Figure 3.** Structural representation of a pentanuclear unit with relevant numbering and intramolecular H bonding between hydroxylmethyl groups of dinuclear units and azido groups of the central anionic species  $[\text{Cu}(\text{N}_3)_4]^{2-}$  (shown by dotted lines) in **1**.

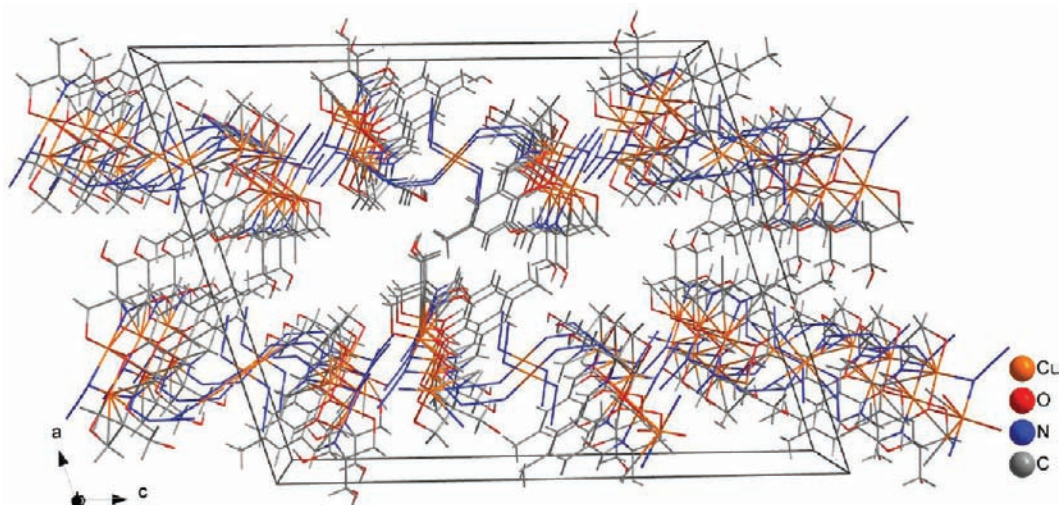


**Figure 4.** Molecular packing of 3D polymeric  $\{[\text{Cu}_2(\text{H}_3\text{L})^{2-}(\text{N}_3)]_2[\text{Cu}(\text{N}_3)_4]\}_n$ .

Structural data for compounds **2** and **3** are very similar, and hence, the structure of **2** is discussed here. The structures of **2** and **3** consist of centrosymmetric hexanuclear neutral cores  $[\text{Ni}_6(\text{H}_3\text{L}^-)_2(\text{HL}2^{2-})_2(\mu\text{-N}_3)_4(\text{X})_2]$  ( $\text{X} = \text{CH}_3\text{CO}_2^-$  (**2**) or  $\text{C}_6\text{H}_5\text{CO}_2^-$  (**3**)) in which four defective cubanes are fused together similar to recently reported hexanuclear nickel(II) clusters.<sup>64,65</sup> The hexanuclear core in each structure involves two singly deprotonated single-Schiff-base ligands ( $\text{H}_4\text{L}^-$ ), two doubly deprotonated tripodal THMAM ( $\text{H}_3\text{L}2^{2-}$ ) ligands, four doubly bridging end-on (EO) ( $\mu\text{-N}_3$ ) azide ions, and two bridging acetate (**2**) or two bridging benzoate (**3**) anions. These results are contrary to our earlier observation,<sup>63,64</sup> where we have seen that the nature of the anion seems to play an important role in directing the self-assembly of the hexanuclear or tetranuclear cluster. In the presence of noncoordinating anions like  $\text{ClO}_4^-$  or

$\text{BF}_4^-$  hexanuclear clusters incorporating two double-Schiff-base ligands and two single-Schiff-base ligands were produced. In the presence of  $\text{CH}_3\text{CO}_2^-$  ions with significant coordinating abilities as monodentate or bidentate ligands a tetranuclear complex involving only two double-Schiff-base ligands ( $\text{H}_3\text{L}$ ) was formed.<sup>64</sup> In our opinion, formation of a double-Schiff-base ligand ( $\text{H}_7\text{L}$ ) as observed in complex **1** or a single-Schiff-base ligand ( $\text{H}_4\text{L}1$ ) as observed in complexes **2** and **3** and the behavior of phenoxide, azide, or alkoxide ions as a bidentate (doubly) or a tridentate (triply) bridges is the result of metal-dictated preferential stereochemical requirements of the metal centers in polynuclear clusters.

In compounds **2** and **3**  $\text{H}_4\text{L}1$  acts as tetradentate ( $\text{NO}_3^-$ ) monoanionic ligand ( $\text{H}_3\text{L}1^-$ ) binding through an imine nitrogen atom, an aldehyde oxygen atom, a protonated alkoxy

oxygen atom of the side arm, and a deprotonated phenoxide oxygen, thereby bridging two nickel(II) ions into a dinuclear unit. Two of the three methanol groups in the side arm of the Schiff-base ligand remain protonated and uncoordinated and are involved in extensive intermolecular hydrogen-bonding interactions producing 3D structures. In each dinuclear unit two nickel(II) ions are bridged through a phenoxide oxygen, an acetate/benzoate group, and a triply bridging deprotonated alkoxide oxygen atom of the H<sub>3</sub>L2 ligand. Perspective views of the neutral hexanuclear units in **2** and **3** with atomic labeling of important atoms are presented in Figures 5 and 6, respectively.

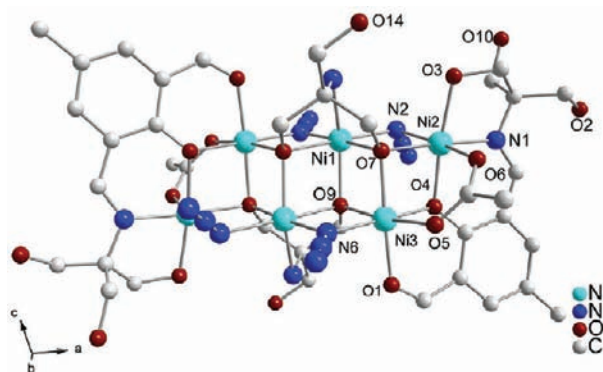


**Figure 5.** Perspective view of a hexanickel core in  $[\text{Ni}_6(\text{H}_3\text{L1}^-)_2(\text{HL}_2^{2-})_2(\text{N}_3)_4(\text{CH}_3\text{CO}_2)_2] \cdot 6\text{C}_3\text{H}_7\text{NO} \cdot \text{C}_2\text{H}_5\text{OH}$  (**2**); six  $\text{C}_3\text{H}_7\text{NO}$  and one  $\text{C}_2\text{H}_5\text{OH}$  molecules presented in the lattice are omitted for clarity.

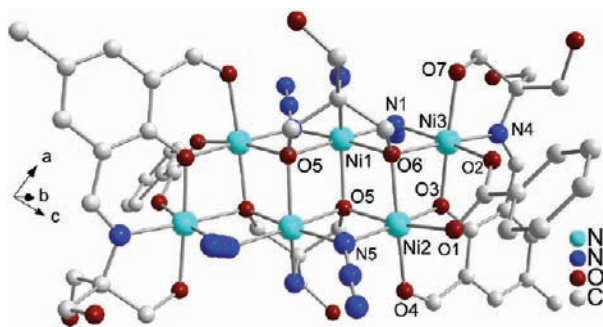


**Figure 6.** Perspective view of a hexanickel core in  $[\text{Ni}_6((\text{H}_3\text{L1}^-)_2(\text{HL}_2^{2-})_2(\text{N}_3)_4(\text{C}_6\text{H}_5\text{CO}_2)_2)] \cdot 3\text{C}_3\text{H}_7\text{NO} \cdot \text{CH}_3\text{OH}$  (**3**); three  $\text{C}_3\text{H}_7\text{NO}$  and one  $\text{CH}_3\text{OH}$  molecules presented in the lattice are omitted for clarity.

The central dinuclear ( $\text{Ni}_2$ ) unit in which two identical symmetry related nickel(II) ions are bridged through two triply bridging deprotonated oxygen atoms of the methanolate arm of the tripodal ligand ( $\text{HL}_2^{2-}$ ) are connected to two terminal dinuclear ( $\text{Ni}_2$ ) units through four doubly bridging EO  $\mu$ -azido (N1, N1) bridges and four triply bridging ( $\mu_3$ -O) alkoxide bridges of two  $\text{HL}_2^{2-}$  ligands organizing into neutral hexanickel units. In **2** and **3**, H<sub>3</sub>L2, potentially a tetradentate ( $\text{NO}_3$ ) trianionic ligand, acts as a tridentate ( $\text{NO}_2$ ) dianionic ligand ( $\text{HL}_2^{2-}$ ) binding through deprotonated oxygen atoms of two of the three methanolate arms and the nitrogen atom of the tripodal ligand. The oxygen atom of the third methanolic arm of H<sub>3</sub>L2 remains protonated and uncoordinated and is involved in intermolecular H-bonding interactions between hexanickel units along the *a* axis, forming a sheet-like structure. Hexanickel units are also interconnected through strong intermolecular

H-bonding interactions between protonated uncoordinated  $-\text{OH}$  groups of H<sub>3</sub>L2 ligands and  $-\text{OH}$  groups of two of the three methanolic side arms of the Schiff-base ligand (H<sub>4</sub>L1) and oxygen atoms of the bridging  $\text{CH}_3\text{CO}_2^-/\text{C}_6\text{H}_5\text{CO}_2^-$  ions along the *b* and *c* axes forming a 3D structure. In addition, there are also H-bonding interactions between noncoordinated  $-\text{OH}$  groups of the H<sub>3</sub>L2 ligands and noncoordinated DMF molecules (Figure 7). The beauty of the ligands used in the

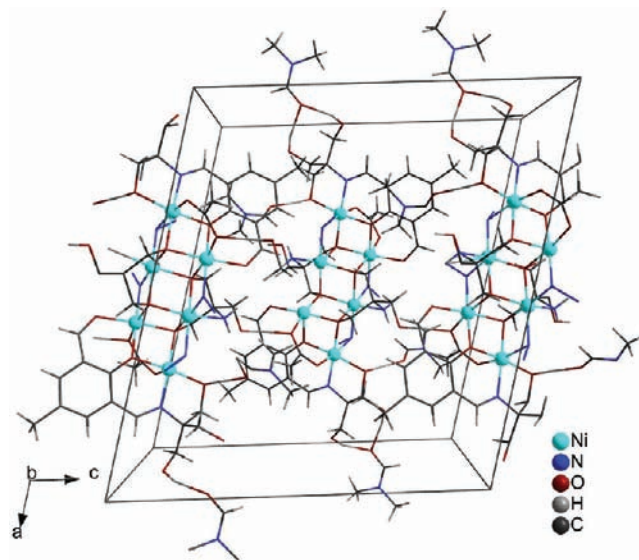


**Figure 7.** Packing diagram for **2** viewed along the *b* axis. Each hexanuclear cluster is hydrogen bonded to adjacent clusters via hydroxyl moieties bound to adjacent carboxylate ligands; each cluster is additionally hydrogen bonded to two DMF molecules.

present study (H<sub>7</sub>L, H<sub>4</sub>L1, H<sub>3</sub>L2) lies in the fact that they have a number of uncoordinated OH groups capable of forming extensive H bonding, thereby stabilizing 3D structures. In biological systems H bonding plays a vital role and is one of the major forces to stabilize the proteins structures.

Relevant bond angles and bond distances for **2** and **3** are given in Tables 3 and 4. The metal–metal distances between Ni(II) ions in terminal dinuclear units is 2.9409 Å, which is significantly shorter than the intermetallic distances observed in most of the similar hexanuclear, tetranuclear, or dinuclear complexes of copper, cobalt, and nickel ions with similar Schiff-base ligands.<sup>57,63–65,69–72</sup> The other metal–metal distances between Ni(II) centers present in the central and terminal dinuclear units lie in the range 3.059–3.122 Å, which are also slightly shorter than the reported distances. The metal–metal separation in the central dinuclear unit is 3.142 Å, which is significantly larger than in the terminal dinuclear units. The stereochemistry at each nickel(II) ion in the terminal dinuclear units [Ni(2) and Ni(3)] can best be described as slightly distorted octahedral with phenoxido O(4), imine N(1), and two methanolic O(3) and O(7) atoms in the equatorial plane and an acetate O(6) and an azido (N(2)) nitrogen in the axial plane at Ni(2) and phenoxido O(4), aldehyde O(1), methanolic O(7), and an azido N(6) atom in the equatorial plane and an acetate O(5) and a methanolic O(9) oxygen in the axial plane at Ni(3) with Ni(2) slightly more distorted than Ni(3). The sum of the bond angles in the basal plane of Ni(2) and Ni(3) are 359.99(10)° and 359.64(10)°, respectively, indicating planar arrangements around these metal centers.



The stereochemical arrangement at Ni(1) of the central dinuclear unit is defined by two methanolic O(7), O(9) oxygen atoms and two azido N(2), N(6) nitrogen atoms in the equatorial plane and a nitrogen N(5) atom and a methanolic O(9) oxygen atom in the axial plane. The sum of the bond angles in the basal plane of Ni(1) is  $360.00(11)^\circ$ , indicating perfectly planar arrangement around Ni(1). The Ni–O and Ni–N bond distances in the basal plane lie in the range 2.014(2)–2.081(3) and 2.017(3)–2.095(3) Å, respectively, and in the axial plane lie in the range  $2.051(2)$ – $2.073(2)^\circ$  and  $2.112(3)$ – $2.135(3)^\circ$ , respectively. In terminal dinuclear (Ni<sub>2</sub>) units the bridge angles at the phenoxide oxygen (O(4)) and triply bridging methoxide oxygen (O(7)) are  $93.42(10)^\circ$  and  $92.56(10)^\circ$ , respectively. In the central dinuclear unit (Ni<sub>2</sub>) the bridge angles at the triply bridging methoxide oxygens (O(9) and O(9A)) of H<sub>3</sub>L2 ligands are  $98.73(10)^\circ$ . The bridging angles at asymmetric doubly bridging azido nitrogens (N(2) and N(6)) and triply bridging methoxide oxygens (O(7) and O(9)) of the H<sub>3</sub>L2 ligand connecting the central dinuclear unit with the terminal dinuclear units are  $95.14(12)^\circ$  (N(2)),  $96.37(13)^\circ$  (N(6)),  $99.89(10)^\circ$  and  $100.85(10)^\circ$  (O(7)), and  $95.29(9)^\circ$  and  $97.46(10)^\circ$  (O(9)), respectively. The sum of the bond angles around the doubly bridging  $\mu$ -phenoxide O(4) atom and two  $\mu$ -azido bridging N atoms, N(2) and N(6), are  $347.92(5)^\circ$ ,  $339.14(6)^\circ$ , and  $359.97^\circ$ , respectively, indicating perfectly planar arrangement at N(6) and significant distortion from planarity at N(2) and O(4) atoms to allow moderately effective magnetic exchange interactions between the Ni(1), Ni(2), and Ni(3) ions in the hexanuclear units. The sum of the bond angles at the  $\mu_3$ -methoxy oxygen (O(7) and O(9)) are  $286.8^\circ$  and  $294.4^\circ$ , respectively, and indicative of pyramidal distortion at these atoms. All azides are almost linear (N–N–N =  $178.2(6)$ – $178.5(4)^\circ$ ). The bridge angles at  $\mu$ -O(4),  $\mu$ -N(2), and  $\mu$ -N(6) of  $93.42^\circ$ ,  $95.14^\circ$ , and  $96.37^\circ$ , respectively, and at  $\mu_3$ -O(7) and  $\mu_3$ -O(9) in the range  $92.56(9)$ – $100.85(10)^\circ$  are providing effective pathways for ferromagnetic interactions between Ni(II) ions in the hexanuclear core.

**Magnetic Properties.** Copper(II) Complex:  $\{[Cu_2(H_5L^2-)(\mu-N_3)]_2[Cu(N_3)_4] \cdot 2CH_3OH\}_n$  (1). Variable-temperature magnetic data for 1 are shown in Figure 8 as plots of susceptibility and

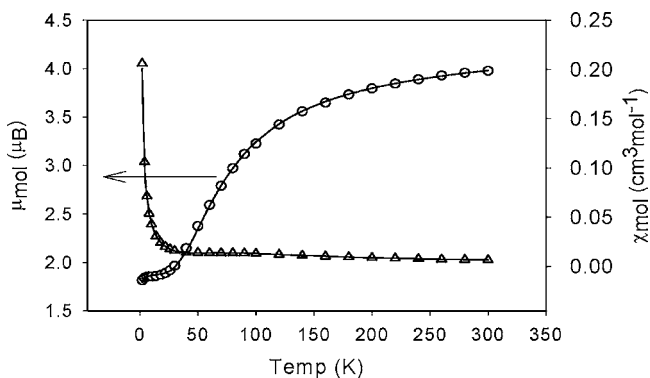
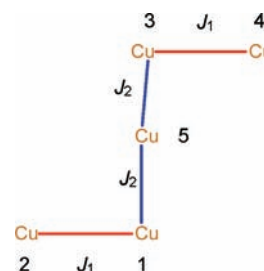


**Figure 8.** Variable-temperature magnetism for 1. Solid lines represent fits to the data. See text for model and parameters.

moment per mole (per pentanuclear unit). The room-temperature moment ( $3.98 \mu_B$ /per pentanuclear unit) is consistent with the presence of two antiferromagnetically coupled Cu(II) ions within each dinuclear unit and drops to  $1.82 \mu_B$  at 2 K, consistent with the odd number of metals present in each pentanuclear unit. A schematic representation of the pentanuclear unit together

with the magnetic coupling exchange pathways is shown in Scheme 3. The following Heisenberg spin Hamiltonian is

**Scheme 3. Schematic Representation and Magnetic Coupling Exchange Pathways in the Pentanuclear Units of 1**



the one corresponding to such a magnetic coupling scheme  $\hat{H} = -J_{12}(\hat{S}_1\hat{S}_2) - J_{15}(\hat{S}_1\hat{S}_5) - J_{35}(\hat{S}_3\hat{S}_5) - J_{34}(\hat{S}_3\hat{S}_4)$  and can be rewritten due to the symmetry relationship between the copper(II) ions as  $\hat{H} = -2J_1(\hat{S}_1\hat{S}_2) - 2J_2(\hat{S}_1\hat{S}_5)$ , where  $J_{12} = J_{34} = J_1$  and  $J_{15} = J_{35} = J_2$ . Magnetic susceptibility data were fitted to this model (solid line), and the best-fit parameters are  $g = 2.14(1)$ ,  $J_1 = -113.5(4) \text{ cm}^{-1}$ ,  $J_2 = 0 \text{ cm}^{-1}$ ,  $TIP = 2.8 \times 10^{-4} \text{ cm}^3 \text{ mol}^{-1}$ , and  $\rho = 0.005$  (fraction paramagnetic impurity). Considering the Cu–O–Cu and Cu(1)–N(3)–Cu(2) bridge angles the two copper ions in the dinuclear units would be expected to take part in a combination of antiferromagnetic and ferromagnetic exchange interactions, with stronger exchange via the phenoxide bridges, as a result of the larger angle. This clearly dominates the overall exchange process and indicates that Cu(1) is coupled directly to Cu(2) through magnetic orbital overlap via the two bridges but not to Cu(5) due to magnetic orbital orthogonality.<sup>22</sup>

**Hexanuclear Nickel(II) Complexes 2 and 3.** The fact that compounds 2 and 3 have quite short Ni–Ni distances (2.9409–3.142 Å) with bridging ligands is likely to result in magnetic interactions. The stereochemistries at the nickel(II) centers in hexanuclear cores are slightly distorted octahedral with almost planar arrangement in the equatorial plane, thus providing effective pathways for magnetic exchange interactions between metal centers. The bridge angles at  $\mu$ -O(4),  $\mu$ -N(2), and  $\mu$ -N(6) of  $93.42^\circ$ ,  $95.14^\circ$ , and  $96.37^\circ$ , respectively, and at  $\mu_3$ -O(7) and  $\mu_3$ -O(9) in the range  $92.56(9)$ – $100.85(10)^\circ$  provide effective pathways for overall ferromagnetic interactions between Ni(II) ions in the hexanuclear core. The temperature dependence of the  $\chi_M T$  product for compounds 2 and 3 is shown in Figure 9 ( $\chi_M$  is the magnetic susceptibility per six Ni(II) ions). At room temperature,  $\chi_M T$  is 8.51 and  $8.36 \text{ cm}^3 \text{ mol}^{-1} \text{ K}$  for 2 and 3 respectively, values which are above the expected values for six magnetically isolated nickel(II) ions [ $\chi_M T = 6(N\beta^2 g^2 / 3kT) S(S+1) = 7.32 \text{ cm}^3 \text{ mol}^{-1} \text{ K}$ , with  $g = 2.21$  and  $S = 1$ ].<sup>22</sup> The  $\chi_M T$  product continuously increases on lowering the temperature, reaching a maximum in both cases, and then decreases at lower temperatures. This behavior indicates an overall ferromagnetic coupling among the nickel(II) ions, and the lowering of  $\chi_M T$  at low temperatures can be due to intermolecular antiferromagnetic coupling and/or a zero-field splitting (zfs) of the ferromagnetically coupled ground-state spin.

The magnetization vs field plot shows saturation values around  $12 N\beta$ , which indicate that the ground state has a  $S = 6$  ground-state spin (Figure 10). This together with the absence of a clear intermolecular magnetic exchange pathway suggests

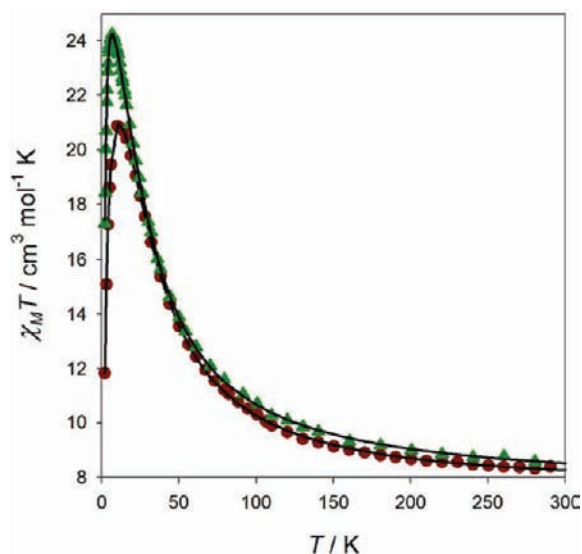


**Figure 9.** Temperature dependence of the  $\chi_M T$  product for compounds 2 (triangles) and 3 (circles). Solid lines correspond to the best fits to the model (see text).

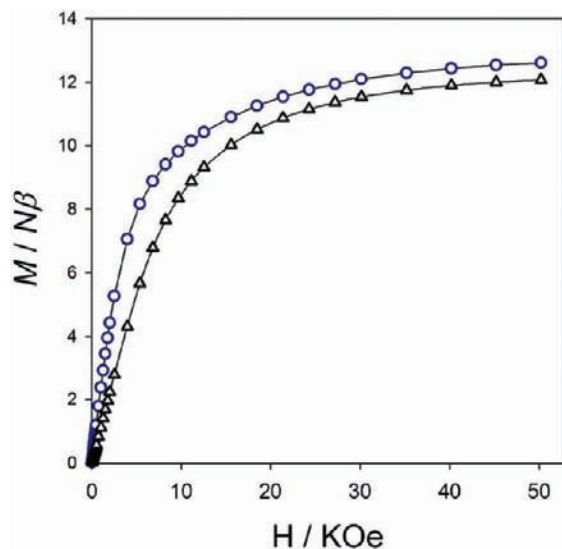


**Figure 10.** Magnetization vs field plot for compounds 2 (circles) and 3 (triangles). Solid lines are guides for the eyes.

that the lowering in the  $\chi_M T$  plot observed at low temperatures is more likely due to a zfs of the  $S = 6$  state. A perspective view of the only coordination core of neutral hexanuclear unit in 2 and 3 is given in Figure 11. The structures of compounds 2 and 3 consist of nickel(II) hexanuclear clusters with equivalent topology, which is depicted in Scheme 4.

For such a system the following zero-field spin Hamiltonian would describe the magnetic behavior.

$$\begin{aligned} \hat{H} = & -J_{12}(\hat{S}_1\hat{S}_2) - J_{23}(\hat{S}_2\hat{S}_3) - J_{34}(\hat{S}_3\hat{S}_4) - J_{45}(\hat{S}_4\hat{S}_5) \\ & - J_{56}(\hat{S}_5\hat{S}_6) - J_{16}(\hat{S}_1\hat{S}_6) - J_{26}(\hat{S}_2\hat{S}_6) - J_{25}(\hat{S}_2\hat{S}_5) \\ & - J_{35}(\hat{S}_3\hat{S}_5) \end{aligned}$$

Analysis of the magnetic data with this spin Hamiltonian would lead to overparameterization in the calculation process; thus, a reduction in the number of variables is necessary. It is

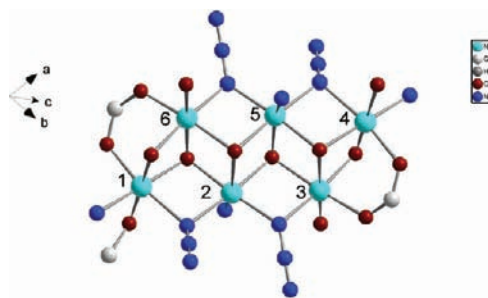
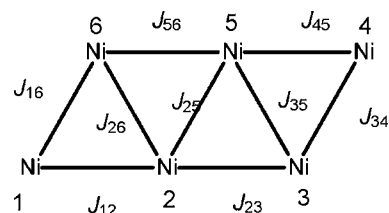


**Figure 11.** Perspective view of only the coordination core of neutral hexanickel units in 2 and 3. H and C atoms of the ligands are omitted.

#### Scheme 4. General Magnetic Coupling Scheme in Compounds 2 and 3



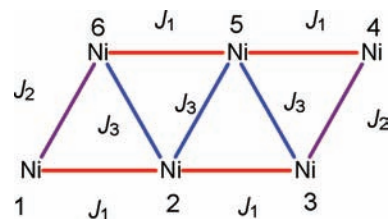
important to find symmetry relationships and structural similarities in order to achieve the reduction. The centers 1, 2, and 3 are symmetry related to 4, 5, and 6, respectively. Moreover, the 1, 2, and 3 centers are bridged by the same bridging groups with similar structural parameters. The bridges between centers 2 and 5, 2 and 6, and the one between 3 and 5 are also very similar. Also, groups bridging 1 and 6 are equivalent to those bridging 3 and 4.

Thus, under this approach the zero-field spin Hamiltonian could be rewritten as

$$\begin{aligned} \hat{H} = & -J_1(\hat{S}_1\hat{S}_2) - J_1(\hat{S}_2\hat{S}_3) - J_2(\hat{S}_3\hat{S}_4) - J_1(\hat{S}_4\hat{S}_5) \\ & - J_1(\hat{S}_5\hat{S}_6) - J_2(\hat{S}_1\hat{S}_6) - J_3(\hat{S}_2\hat{S}_6) - J_3(\hat{S}_2\hat{S}_5) \\ & - J_3(\hat{S}_3\hat{S}_5) \end{aligned}$$

Thus, we made  $J_{12} = J_{23} = J_{45} = J_{56} = J_1$ ,  $J_{16} = J_{34} = J_2$ , and  $J_{26} = J_{25} = J_{35} = J_3$ . This situation is shown in Scheme 5.

#### Scheme 5. Reduced Magnetic Coupling Scheme in Compounds 2 and 3



A reduction in the number of variables can now allow determination of the magnetic coupling constants. The magnetic susceptibility data have been analyzed with the MAGPACK software, and the results are shown in Table 5. [ $R$  is the agreement factor defined as  $\sum_i [(\chi_M T)_{\text{obs}}(i) - (\chi_M T)_{\text{calcd}}(i)]^2 / \sum_i [(\chi_M T)_{\text{obs}}(i)]^2$ .] A zero-field-splitting parameter has been considered for the decrease of  $\chi_M T$  at low temperatures. The magnetic coupling is found to be ferromagnetic for all bridges, and the values obtained for compound 2 are comparable with

Table 5. Best-Fit Parameters for Compounds 2 and 3

	$J_1$ (cm <sup>-1</sup> )	$J_2$ (cm <sup>-1</sup> )	$J_3$ (cm <sup>-1</sup> )	$g$	$ D $ (cm <sup>-1</sup> )	$R$
compound 2	2.10	14.56	7.57	2.23	2.02	$1.48 \times 10^{-5}$
compound 3	4.01	4.28	10.51	2.18	18.29	$8.65 \times 10^{-6}$

those observed in compound 3. The bridge between 1 and 2, 2 and 3, 4 and 5, and 5 and 6 centers consists of a  $\mu_3$ -alkoxide and a  $\mu$ -N<sub>3</sub><sup>-</sup> which have been observed to mediate ferromagnetic coupling<sup>24,65</sup> with similar values in other systems. The *syn-syn* carboxylate bridge together with  $\mu_3$ -alkoxide bridges have been observed to mediate ferromagnetic coupling due to orbital countercomplementarity phenomenon,<sup>73–76</sup> so the value observed is as expected. Finally, the  $\mu_3$ -alkoxide bridge has also been observed to mediate weak ferromagnetic coupling in other Ni<sub>6</sub> clusters,<sup>65</sup> so the ferromagnetic interactions for all of the pairings defined in complexes 2 and 3 are not unexpected. The value obtained for the *zfs* in complex 2 is in the expected range; however, the one found in 3 is much higher than the expected value, and this may indicate the presence of some intermolecular antiferromagnetic exchange interactions. Single-crystal X-ray analysis of 2 and 3 shows the presence of strong intermolecular H-bonding interactions directing self-assembly of 3D structures. We introduced a *zj'* term in our calculation, but it has not been possible to improve the result due to over parametrization problems, so the value obtained for  $|D|$  must be considered as a tentative upper limit contaminated with some antiferromagnetic interactions among the Ni<sub>6</sub> clusters.

Highly anisotropic and well-isolated ferromagnetically coupled polymetallic clusters may exhibit single-molecule magnet (SMM) behavior; in this sense *ac* magnetic measurements have been performed for compounds 2 and 3 in order to explore this possibility. However, positive values for the out-of-phase magnetic susceptibility have not been observed, which indicates that 2 and 3 do not behave as SMM.

## CONCLUSIONS

Metal-catalyzed template synthesis of two new Schiff-base ligands, H<sub>7</sub>L (double Schiff base) and H<sub>4</sub>L1 (single Schiff base), with a very high degree of conformational flexibility and potential to coordinate in a convergent and a divergent fashion, have been achieved, and their coordination potentials toward Cu(II) and Ni(II) ions have been explored. In a single pot, reactions between DFMP and THMAM in the presence of any copper(II) salt and NaN<sub>3</sub> under varied conditions always formed a polymeric copper(II) complex consisting of pentanuclear copper(II) units (1) which organizes into a double-helical ladder-like structure. When the same reaction was carried out in the presence of Ni(CH<sub>3</sub>CO<sub>2</sub>)<sub>2</sub> and Ni(ClO<sub>4</sub>)<sub>2</sub>/C<sub>6</sub>H<sub>5</sub>CO<sub>2</sub><sup>-</sup>, NaN<sub>3</sub> and TEA, it resulted in formation of neutral hexanuclear Ni(II) complexes 2 and 3, respectively, involving H<sub>4</sub>L1 and H<sub>3</sub>L2 ligands along with four  $\mu$ -N<sub>3</sub> bridges. Formation of H<sub>4</sub>L1 present in 2 and 3 has been assigned either to nickel-catalyzed partial hydrolysis of originally formed double-Schiff-base ligand H<sub>7</sub>L or to the preferential stereochemical requirements of nickel(II) centers in hexanuclear units. The methanol groups in the side arms of H<sub>7</sub>L, H<sub>4</sub>L1, and tripodal arms of H<sub>3</sub>L2 ligands undergo various degrees of deprotonation depending upon the charge requirement of the resulting complexes. The uncoordinated and protonated methanol groups in the side arms of the ligands are involved in intramolecular and intermolecular H-bonding interactions forming 3D structures in all three complexes (1–3). Considering the Cu–O–Cu and

Cu(1)–N(3)–Cu(2) bridge angles, the magnetic coupling in 1 is dominated by the strong antiferromagnetic interaction within the [Cu<sub>2</sub>] moieties. The magnetic couplings between Ni(II) ions in neutral hexanuclear cores in 2 and 3 are found to be ferromagnetic for all bridges. Further studies involving reactions of DFMP and THMAM in the presence of various 3d and 4f metal ions and mixed metal 3d–4f metal ions under varied conditions to produce coordination compounds of high nuclearity with high ground spin state and potential application in magnetic materials are in progress.

## ASSOCIATED CONTENT

### Supporting Information

X-ray crystallographic files in CIF format for the structures of 1–3. This material is available free of charge via the Internet at <http://pubs.acs.org>. Crystallographic data (excluding structure factors) for the structures have been deposited with the Cambridge Crystallographic Data Centre as supplementary publication nos. CCDC 722737, CCDC 853782, and CCDC 853783 for 1, 2, and 3, respectively. Copies of the data can be obtained, free of charge, on application to CCDC, 12 Union Road, Cambridge CB2 1EZ, UK (fax, +44-(0)1223-336033; e-mail, [deposit@ccdc.cam.ac.uk](mailto:deposit@ccdc.cam.ac.uk)).

## AUTHOR INFORMATION

### Corresponding Author

\*E-mail: [standon@kent.edu](mailto:standon@kent.edu).

### Notes

The authors declare no competing financial interest.

## ACKNOWLEDGMENTS

Kent State University—Salem is thanked for financial support, and S.S.T. thanks Professor Roger Gregory, Chemistry Department, Kent State University at the Kent Campus (KSU), for laboratory facilities and Dr. Mohinda Gandogora (KSU) for assistance with spectroscopic and analytical studies. L.K.T. thanks NSERC (Canada) for financial support.

## REFERENCES

- Brechin, E. K.; Boskovic, C.; Wernsdorfer, W.; Yoo, J.; Yamaguchi, A.; Sanudo, E. C.; Concolino, T. R.; Rheingold, A. L.; Ishimoto, H.; Hendrickson, D. N.; Christou, G. *J. Am. Chem. Soc.* **2002**, *124*, 9710–9711.
- Friedman, J. R.; Sarachik, M. P.; Tejada, J.; Maciejewski, J.; Ziolo, R. *J. Appl. Phys.* **1996**, *79*, 6031–6033.
- Friedman, J. R.; Sarachik, M. P.; Tejada, J.; Ziolo, R. *Phys. Rev. Lett.* **1996**, *76*, 3830–3833.
- Gatteschi, D.; Sessoli, R. *Angew. Chem., Int. Ed.* **2003**, *42*, 268–297.
- Sessoli, R.; Gatteschi, D.; Caneschi, A.; Novak, M. A. *Nature* **1993**, *365*, 141–143.
- Sessoli, R.; Tsai, H. L.; Schake, A. R.; Wang, S. Y.; Vincent, J. B.; Folting, K.; Gatteschi, D.; Christou, G.; Hendrickson, D. N. *J. Am. Chem. Soc.* **1993**, *115*, 1804–1816.
- Thomas, L.; Lioni, F.; Ballou, R.; Gatteschi, D.; Sessoli, R.; Barbara, B. *Nature* **1996**, *383*, 145–147.
- Bagai, R.; Wernsdorfer, W.; M., L.-G.; Christou, G. *J. Am. Chem. Soc.* **2007**, *129*, 12918–20.



- (9) Gatteschi, D.; Sessoli, R. *J. Magn. Magn. Mater.* **2004**, 272–76, 1030–1036.
- (10) Milios, C. J.; Vinslava, A.; Wernsdorfer, W.; Moggach, S.; Parsons, S.; Perlepes, S. P.; Christou, G.; Brechin, E. K. *J. Am. Chem. Soc.* **2007**, 129, 2754–55.
- (11) Milios, C. J.; Vinslava, A.; Wood, P. A.; Parsons, S.; Wernsdorfer, W.; Christou, G.; Perlepes, S. P.; Brechin, E. K. *J. Am. Chem. Soc.* **2007**, 129, 8–9.
- (12) Murugesu, M.; Habrych, M.; Wernsdorfer, W.; Abboud, K. A.; Christou, G. *J. Am. Chem. Soc.* **2004**, 126, 4766–4767.
- (13) Soler, M.; Wernsdorfer, W.; Folting, K.; Pink, M.; Christou, G. *J. Am. Chem. Soc.* **2004**, 126, 2156–2165.
- (14) Stamatatos, T. C.; Abboud, K. A.; Wernsdorfer, W.; Christou, G. *Angew. Chem., Int. Ed.* **2007**, 46, 884–888.
- (15) Yang, E. C.; Hendrickson, D. N.; Wernsdorfer, W.; Nakano, M.; Zakharov, L. N.; Sommer, R. D.; Rheingold, A. L.; Ledezma-Gairaud, M.; Christou, G. *J. Appl. Phys.* **2002**, 91, 7382–7384.
- (16) Aliaga-Alcalde, N.; Edwards, R. S.; Hill, S. O.; Wernsdorfer, W.; Folting, K.; Christou, G. *J. Am. Chem. Soc.* **2004**, 126, 12503–12516.
- (17) Caneschi, A.; Gatteschi, D.; Lalioti, N.; Sangregorio, C.; Sessoli, R.; Venturi, G.; Vendigni, A.; Retoori, A.; Pini, M. G.; Novak, M. A. *Angew. Chem., Int. Ed.* **2001**, 40, 1760–1763.
- (18) Clerac, R.; Miyasaka, H.; Yamashita, M.; Coulon, C. *J. Am. Chem. Soc.* **2002**, 124, 12837–12844.
- (19) Coulon, C.; Clerac, R.; Lecren, L.; Wernsdorfer, W.; Miyasaka, H. *Phys. Rev. B* **2004**, 69.
- (20) Coulon, C.; Miyasaka, H.; Clerac, R. *Struct. Bonding (Berlin)* **2006**, 122, 163–206.
- (21) Milios, C. J.; Inglis, R.; Vinslava, A.; Bagai, R.; Wernsdorfer, W.; Parsons, S.; Perlepes, S. P.; Christou, G.; Brechin, E. K. *J. Am. Chem. Soc.* **2007**, 129, 12505–12511.
- (22) Kahn, O. *Molecular Magnetism. Molecular Magnetism*; VCH: New York, 1993; p 131.
- (23) Miller, J. S.; Epstein, A. J. *Angew. Chem., Int. Ed.* **1994**, 33, 385–415.
- (24) Ribas, J.; Escuer, A.; Monfort, M.; Vicente, R.; Cortes, R.; Lezama, L.; Rojo, T. *Coord. Chem. Rev.* **1999**, 195, 1027–1068.
- (25) Thompson, L. K. *Coord. Chem. Rev.* **2002**, 233, 193–206.
- (26) Turnbull, M. M.; Sugimoto, T.; Thompson, L. K. *Molecule-Based Magnetic Materials—Theory, Techniques, And Applications*; American Chemical Society: Washington, DC, 1996; Vol. 644.
- (27) Christou, G.; Gatteschi, D.; Hendrickson, D. N.; Sessoli, R. *MRS Bull.* **2000**, 25, 66–71.
- (28) Miller, J. S.; Drillon, M. *Magnetism: Molecules to Materials*; Wiley: Weinheim, 2001.
- (29) Wernsdorfer, W.; Sessoli, R. *Science* **1999**, 284, 133–135.
- (30) Du, M.; Guo, Y. M.; Bu, X. H. *J. Chem. Cryst.* **2002**, 32, 127.
- (31) Hu, D. H.; Huang, W.; Cui, K.; Li, Y. Z.; Gou, S. H.; Yan, J. L. *Acta Crystallogr.* **2004**, C60, m91–m93.
- (32) Wang, G. H.; Li, Z. G.; Xu, J. W.; Hu, N. H. *Acta Crystallogr.* **2007**, E63, m289–m291 and the references therein.
- (33) He, H.; Dai, F.; Xie, A.; Tong, X.; Sun, D. *CrystEngComm* **2008**, 10, 1429–1435.
- (34) Rao, C. N. R.; Natarajan, S.; Choudhury, A.; Neeraj, S.; Ayi, A. *Acc. Chem. Res.* **2001**, 34, 80–87 and the references therein.
- (35) Huh, H. S.; Min, D.; Lee, Y. K.; Lee, S. W. *Bull. Korean Chem. Soc.* **2002**, 23, 619.
- (36) Escuer, A.; Aromi, G. *Eur. J. Inorg. Chem.* **2006**, 4721–4736.
- (37) Ferbinteanu, M.; Miyasaka, H.; Wernsdorfer, W.; Nakata, K.; Sugiura, K.; Yamashita, M.; Coulon, C.; Clerac, R. *J. Am. Chem. Soc.* **2005**, 127, 3090–3099.
- (38) Massoud, S. S.; Mautner, F. A.; Vicente, R.; Gallo, A. A.; Ducasse, E. *Eur. J. Inorg. Chem.* **2007**, 1091–1102.
- (39) Tasiopoulos, A. J.; Vinslava, A.; Wernsdorfer, W.; Abboud, K. A.; Christou, G. *Angew. Chem., Int. Ed.* **2004**, 43, 2117–2121.
- (40) Chakov, N. E.; Wernsdorfer, W.; Abboud, K. A.; Christou, G. *Inorg. Chem.* **2004**, 43, 5919–5930.
- (41) Ribas, J. R. I. *Contrib. Sci.* **1999**, 1, 39–51.
- (42) Charlot, M. F.; Kahn, O.; Chaillet, M.; Larrieu, C. *J. Am. Chem. Soc.* **1986**, 108, 2574–2581.
- (43) Thompson, L. K.; Tandon, S. S. *Comm. Inorg. Chem.* **1996**, 18, 125–144.
- (44) Meyer, F.; Kozłowski, H. In *Comprehensive Coordination Chemistry*; McCleverty, J. A., Meyer, T. J., Eds.; Pergamon: New York, 2004; pp 247–276.
- (45) Boudalis, A. K.; Donnadiu, B.; Nastopoulos, V.; Clemente-Juan, J. M.; Mari, A.; Sanakis, Y.; Tuchagues, J. P.; Perlepes, S. P. *Angew. Chem., Int. Ed.* **2004**, 43, 2266–2270.
- (46) Nanda, P. K.; Aromi, G.; Ray, D. *Chem. Commun.* **2006**, 3181–3183.
- (47) Demeshko, S.; Leibel, G.; Maringgele, W.; Meyer, F.; Mennerich, C.; Klaus, H. H.; Pritzkow, H. *Inorg. Chem.* **2005**, 44, 519–528.
- (48) Meyer, F.; Demeshko, S.; Leibel, G.; Kersting, B.; Kaifer, E.; Pritzkow, H. *Chem.—Eur. J.* **2005**, 11, 1518–1526.
- (49) Meyer, F.; Kozłowski, H. In *Comprehensive Coordination Chemistry*; McCleverty, J. A., Meyer, T. J., Eds.; Pergamon: New York, 2004; pp 247–276.
- (50) Halcrow, M. A.; Huffman, J. C.; Christou, G. *Angew. Chem., Int. Ed.* **1995**, 34, 889–891.
- (51) Halcrow, M. A.; Sun, J. S.; Huffman, J. C.; Christou, G. *Inorg. Chem.* **1995**, 34, 4167–4177.
- (52) Ma, D. Q.; Hikichi, S.; Akita, M.; Moro-oka, Y. *J. Chem. Soc., Dalton Trans.* **2000**, 7, 1123–1134.
- (53) Kessissoglou, D. P.; Kirk, M. L.; Lah, M. S.; Li, X.; Raptopoulou, C.; Hatfield, W. E.; Pecoraro, V. L. *Inorg. Chem.* **1992**, 31, 5424.
- (54) Dey, M.; Rao, C. P.; Saarenketo, P. K.; Rissanen, K. *Inorg. Chem. Commun.* **2002**, 5, 380.
- (55) Tsapkov, V. I.; Chumakov, Y. M.; Antosyak, B. Y.; Bocelli, G.; Samus, N. M.; Gulya, A. P. *Koord. Kim. (Russ.)* **2004**, 30, 288.
- (56) Chumakov, Y. M.; Tsapkov, V. I.; Simonov, Y. A.; Antosyak, B. Y.; Bocelli, G.; Perin, M.; Starikova, Z. A.; Samus, N.; Gulya, A. P. *Koord. Kim. (Russ.)* **2005**, 31, 621.
- (57) Tandon, S. S.; Bunge, S. D.; Patel, N.; Thompson, L. K. *Inorg. Chem. Commun.* **2009**, 12, 1077–1080.
- (58) Ullman, F.; Brittner, K. *Chem. Ber.* **1909**, 42, 2539–2549.
- (59) Liu, H. F.; Zhang, X. Q.; Bai, X. Q.; Chen, S. Y.; Shen, X. S. *Chem. J. Internet* **2008**, 10, 34.
- (60) Bruker, A. SAINT 6.45A; Bruker Analytical X-ray Systems: Gottingen, Germany, 2003, 6.
- (61) Bruker, A. APEX II V6.12; Analytical X-ray Systems; Gottingen, Germany, 2005; II.
- (62) Bruker, A. SHELXTL V6.12; Analytical X-ray Systems: Gottingen, Germany, 2002; Vol. 6.
- (63) Tandon, S. S.; Bunge, S. D.; Motry, D.; Costa, J. S.; Aromi, G.; Reedijk, J.; Thompson, L. K. *Inorg. Chem.* **2009**, 48, 4873–4881.
- (64) Tandon, S. S.; Bunge, S. D.; Rakosi, R.; Xu, Z.; Thompson, L. K. *Dalton Trans.* **2009**, 6536–6551.
- (65) Mandal, D.; Bertolasi, V.; Ribas-Arino, J.; Aromi, G.; Ray, D. *Inorg. Chem. Commun.* **2008**, 47, 3465–3467.
- (66) Shiga, T.; Maruyama, K.; Han, L. Q.; Oshio, H. *Chem. Lett.* **2005**, 34, 1648–1649.
- (67) Yamashita, S.; Shiga, T.; Kurashina, M.; Nihei, M.; Nojiri, H.; Sawa, H.; Kakiuchi, T.; Oshio, H. *Inorg. Chem.* **2007**, 46, 3810–3812.
- (68) Thompson, L. K.; Tandon, S. S.; Manuel, M. E.; Park, M. K.; Handa, M. Magnetostructural correlations in dinuclear Cu(II) and Ni(II) complexes bridged by  $\mu$ -1,1-azide and  $\mu$ -phenoxide. In *Molecule-Based Magnetic Materials—Theory, Techniques, and Applications*; Turnbull, M. M., Sugimoto, T.; Thompson, L. K., Eds.; American Chemical Society: Washington, DC, 1996; Vol. 644, pp 170–186.
- (69) Mandal, D.; Ray, D. *Inorg. Chem. Commun.* **2007**, 10, 1202–1205.
- (70) Mukherjee, S.; Weyhermuller, T.; Bothe, E.; Chaudhuri, P. *Eur. J. Inorg. Chem.* **2003**, 1956–1965.
- (71) Mukherjee, S.; Weyhermuller, T.; Bothe, E.; Wiegardt, K.; Chaudhuri, P. *Eur. J. Inorg. Chem.* **2003**, 863–875.

(72) Zhang, W. X.; Ma, C. Q.; Wang, X. N.; Yu, Z. G.; Lin, Q. J.; Jiang, D. H. *Chin. J. Chem.* **1995**, *13*, 497–503.

(73) El Fallah, M. S.; Vicente, R.; Escuer, A.; Badyine, F.; Solans, X.; Font-Bardia, M. *Inorg. Chim. Acta* **2008**, *361*, 4065–4069.

(74) Nishida, Y.; Kida, J. *J. Chem. Soc., Dalton Trans.* **1986**, 2633.

(75) McKee, V.; Zvagulis, M.; Reed, C. A. *Inorg. Chem.* **1985**, *24*, 2914.

(76) Fabelo, O.; Cañadillas-Delgado, L.; Pasán, J.; Delgado, F. S.; Lloret, F.; Cano, J.; Julve, M.; Ruiz-Pérez, C. *Inorg. Chem.* **2009**, *48*, 11342–11351.